BALANCING CONTROL AND NAVIGATION CONTROL FOR QUADRUPED ROBOT

by

Tanzeel Ahmad Fazal

A Thesis Submitted in Partial Fulfillment of the Requirements for the Degree of Master of Engineering in Mechatronics

Examination Committee:	Prof. Manukid Parnichkun (Chairperson)
	Dr. Pisut Koomsap
	Dr. Mongkol Ekpanyapong
Nationality:	Pakistani
Previous Degree:	Bachelor of Science in Mechatronics Engineering
	University of Engineering and Technology
	Taxila, Pakistan
Scholarship Donor:	His Majesty the King's Scholarships (Thailand)

Asian Institute of Technology
School of Engineering and Technology
Thailand
May 2021

AUTHOR'S DECLARATION

I, Tanzeel Ahmad Fazal, declare that the research work carried out for this thesis was in accordance with the regulations of the Asian Institute of Technology. The work presented in it are my own and has been generated by me as the result of my own original research, and if external sources were used, such sources have been cited. It is original and has not been submitted to any other institution to obtain another degree or qualification. This is a true copy of the thesis, including final revisions.

Date: May,2021

Name: TANZEEL AHMAD FAZAL

Signature:

ACKNOWLEDGEMENTS

Firstly, I would like to be deeply grateful to Prof. Manukid Parnichkun for being my advisor and giving me valuable suggestions and guidance throughout this research. I would like to be especially thankful to him for guiding me to select a good research topic which enabled me to learn in depth about mechatronics engineering.

My sincere appreciation goes to Dr. Pisut Koomsap and Dr. Mongkol Ekpanyapong for contributing their valuable time, suggestions and being my examination committee.

I would like to express my deepest gratitude towards my family, especially for my father, for providing continuous support and motivation throughout my education.

I am also thankful for Mr. Hoang Hung Manh for facilitating me from the beginning of this project till the last moment.

ABSTRACT

Nowadays in advanced robotics, mobile robots including legged as well as wheeled have become most interesting research topic. Meanwhile, Legged robots have more future in coming days because of its capabilities to survive in challenging rough terrains and can avoid obstacles more conveniently instead of wheeled robots. However, in near future legged robots will replace all the workers in hazardous environment for human safety and will assist different official organizations including military and bomb disposal forces to do their tasks remotely or autonomously.

The developed robotic system used four legs having 3 degree of Freedoms in each leg for motion. Trotting gait pattern is faster and better for dynamic stability as compared to other gait patterns i.e., static walking and amble gait. Moreover, stability control is also essential during dynamic mobility of robot. Hence, modeled as biped robot for stability with massless and zero inertia of the leg. But in real environment, these factors effects significantly.

Linear robust control is implemented for gait tracking and sideways disturbances retrieval when external forces applied. Sideways disturbances retrieval (SDR) can be defined as the position of legs in free gait pattern to retrieve its body against sideways disturbances. Proposed control is mixed H2/H∞ robust controller in structure of PID as well as the Zero Moment Point (ZMP) balancing technique is adopted to balance the body during trotting.

For navigation control, an open loop approximation method has adopted, and robot can move remotely as well as autonomously. Consequently, results confirms that robust control for dynamic stability during trotting and sideways disturbances retrieval performs well. And navigation control has minor errors due to open loop system.

CONTENTS

LIST OF TABLES

Tables **Page**

LIST OF FIGURES

Figures **Page**

LIST OF ABBREVIATIONS

CAD	= Computer Aided Drawing
AI	= Artificial Intelligence
RPM	= Revolutions Per Minute
COG	= Center of Gravity
I/O’s	= Inputs / Outputs
COM	= Center of Mass
ZMP	= Zero Moment Point
HMI	= Human Machine Interface
PID	= Proportional Integral Derivation
DOF	= Degree of Freedom
ROS	= Robotic Operating System

CHAPTER 1
INTRODUCTION

1.1 Motivation

Nowadays in Advanced Robotics, mobile robots including legged and wheeled have become most interesting research topic. Meanwhile, Legged robots have more future in coming days because of its capabilities to survive in challenging rough terrains and can avoid obstacles more conveniently instead of wheeled robots. However, in near future legged robots will replace all the workers in hazardous environment and will assist different official organizations including military and bomb disposal forces to do their tasks remotely or autonomously.

Legged robotics including biped, quadruped and multi-legged robots, while biped and quadruped are basically two more focusing areas on legged robotics. And in sense of stability, quadruped robots can more stable than biped as well as more concise and adaptive in surrounding environment as compared to multi-legged robots (Li, et al., 2013).

Most important reason of becoming this research topic more popular is its adaptability and flexibility with the environment. Many research industries have built quadruped robots for different tasks including transporting materials, operations in underground mines and unapproachable places by humans as well as for battlefields. These robots have dual functionality either can operate in remote control mode or in autonomous mode. Moreover, legged robots have advantages over wheeled robots as mentioned below.

- Legged robots can traverse any rough and extremely amorphous environment.
- They are adaptable than wheeled robots and have greater edge in navigation control.
- Legged robots can jump and step on any obstacle unlike wheeled robots, hence wheeled robots need to adopt other path to overcome obstacle.
- Legged robots facilitate us to explore the walking way of different species.

The proposed robotic system uses four legs having 3 degree of Freedoms in each leg for walking. Hence, it would require a robust controlling algorithm for balancing itself. Considering past research, many controlling techniques including PID, Fuzzy Controllers and coordinate based approaches in (Lakatos, et al., 2019) have presented for balancing the robots. Moreover, proposed robotic system have 3 revolute joints i.e., one in hip, one for thigh and one revolution for shank for all four legs to walk and balance this quadruped system. Hence, we would present a robust controlling approach as well as the navigation control for our quadruped robot.

1.2 Problem Statement

Practical implementation of quadruped robot is very challenging task as compared to the ideal virtual environment. The real time environment is strained and more complex because of inauspicious effects from irregular ground surfaces and lateral affects, may cause for unstable due to forces of foot contact and unbalance of whole body. Therefore, legged robotics need to tackle more challenging environment for balancing control.

For mechanical aspects, both hind-legs and fore-legs should have same design to minimize the control system's adversity. Proposed system uses four legs for walking on flat surfaces, thus we need to consider the dynamics of the system to maintain the balance throughout walking as well as lateral forces impacts that cause robots to lose its stability.

The thesis will focus to cover the robust control against sideway forces for quadruped robot and robust controlling technique in static balancing and dynamic balancing during walking by shifting center of gravity (COG) of the system as well as the navigation control.

1.3 Objectives of Research

- To develop the robust control for balancing and tracking of gait cycle as well as the control against environmental disturbance forces of four-legged robot.
- To develop autonomous algorithm for navigation in unstable and amorphous environment.

For practical implementation, Platform is being used with the following specifications.

1. The robot has height about 400 mm, length of 400 mm and width of 280 mm.
2. The robot has total 12 degree of freedoms (3 degree of freedoms in each leg).
3. The robot would be able to walk with speed of 0.5 - 0.6m / sec.

1.4 Scope and Limitations of the Research

1.4.1 Scope of Study

1. The robot would be able to walk on flat surfaces as well as rough terrain.
2. The robot will develop with self-balancing control and robust against disturbances.
3. The robot will develop with autonomous navigation as well as remotely controlled.

1.4.2 Limitation of Study

1. The robot would be able to walk on inclined surfaces with maximum inclination of 20°.
2. The robot can upstand with maximum force of 10-12 N in longitudinal and lateral direction (x and y axes) as well as force of 12-15 N in vertical direction.

CHAPTER 2
LITERATURE REVIEW

Two main areas covered in literature review chapter are mentioned below.

1. Mechanical designs of quadruped robots.
2. Balancing controls of legged robots.

2.1 Mechanical Designs of Quadruped Robots

Four-legged robots can be divided into two categories, sprawling or mammal-type. In sprawling-type, the leg configuration is such that in standard posture, its first upper leg section (thigh) is in x-axis (horizontal) and lower section (shank) is in y-axis (vertical) direction as shown in fig a. While for mammals-type leg configuration in standard pose, the foots located vertically downward from bottom of leg as shown in fig b.

Figure 2.1

Two Configurations of Legged Robot

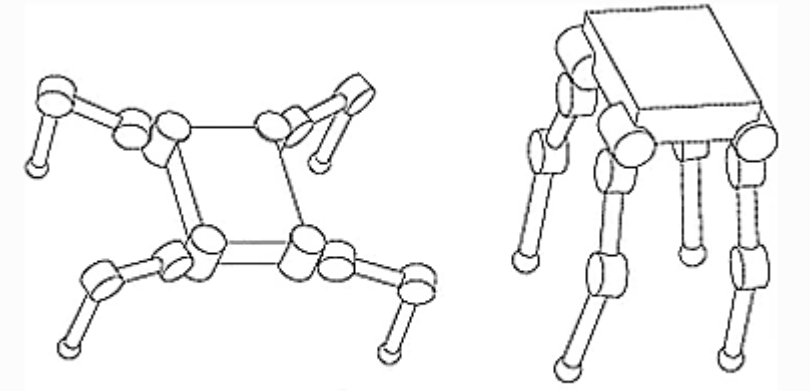

Fig (a) Fig (b)

Both categories have their own features and limitations in term of speed, stability, and control.

2.1.1 Sprawling-Type Quadruped Robot

Sprawling mode of legged robot has features including high stability, low center of gravity, larger leg polygon, and adaptability. Following to this, just elaborate the selective features in a way. The robot can trace its center of gravity at low position; hence the stability of the robot is high as well as due to larger favoring polygon of leg

(Kitano, 2016). So far, many researchers have developed sprawling type robots for doing research on mechanical stability and control techniques. Following are the developed robot which reported high adaptability in rough terrain.

SILO4 (Garcia & Santos, 2006) having sprawling type configuration, created by using spiroid gears with compact leg to walk and they used the force sensors in all feet as well as it can carry a load of 50-N. This robot has developed to maximize the robustness of walking in tough or bumpy environment. Moreover, they have attempted to increase the gait speed as well as to improve the response against the external disruptions or forces. SILO4 is presented in figure 2.2.

Figure 2.2

SILO4 Robot (Garcia & Santos, 2006)

Quadruped robot developed at UTEC (F. García-Cárdenas, 2020) by researchers used a ROS framework for autonomous navigation and path planning. The prototype consisted of four legs with 3 DOF on each leg to minimize the singularity conditions. The chassis consisted of 3D printing parts to make it light weight and feasible structure. Researchers used the NIVIDA Jetson to control the system containing 12 servo motors being driven by drivers PCA9685. To monitor and control this quadruped robot, they developed an HMI using Linux OS. Hence purpose of this robot to reduce the cost and to maximize the performance. Moreover, for new developers or beginners to understand the basic learning tools of ROS and controlling the four-legged robots.

Figure 2.3

Quadruped Robot of UTEC (F. García-Cárdenas, 2020)

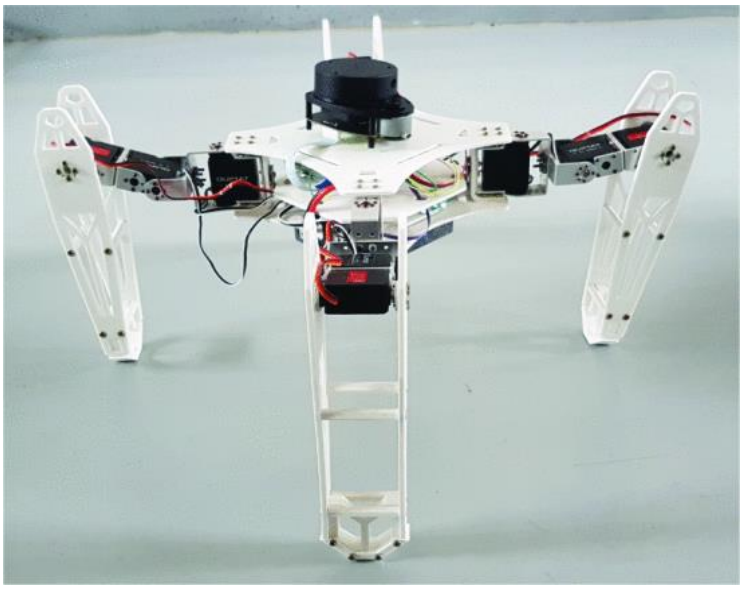

MRWALL-SPECT IV (Vo-Gia Loc, 2012) introduced for pertinency in locomotion and workspace of body. Researchers worked on determination of the possible body positions in uneven terrain and the model used lower (shank) and upper (thigh) links of equal lengths at equidistant with 3 DOF on each leg. In addition, they have successfully reduced the singularity conditions and implemented the concept of body workspace. Hence, achieved the successful walking on rough surfaces.

Figure 2.4

MR4 Quadruped (Vo-Gia Loc, 2012)

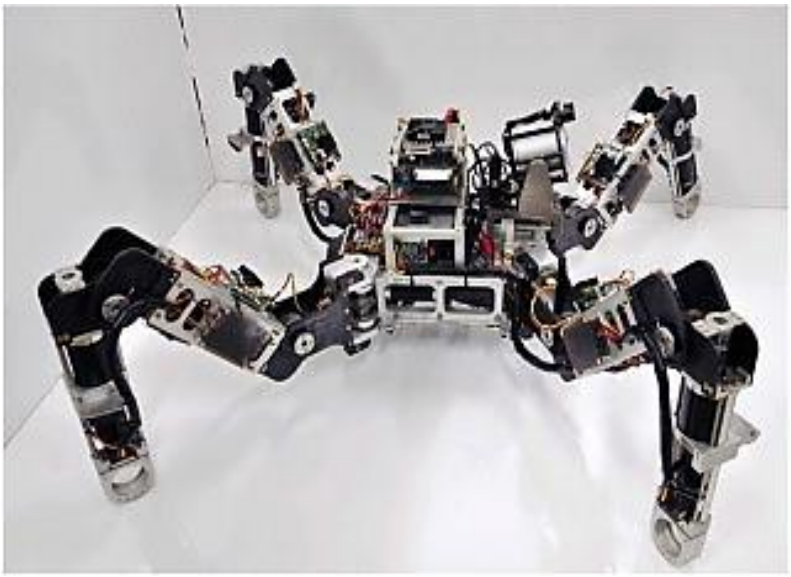

Pneumatic actuated legged robot (Wait & Goldfarb, 2014) built for presenting the optimize mechanical hardware and control of pneumatic based robot as well as to maximize the performance. Pneumatic based robot had a central spine with four legs and each leg had 3 leg segments and 3 DOF. Robot was driven by liquid propellant (H_2O_2) as a fuel for pneumatic cylinders instead of battery power source. Developed robot used potentiometer (ALPS RDC503013A) in each leg joint to measure the joint angles and load cells to get force signals were installed between pneumatic actuators (Wait, Dalley, & Goldfarb, Design and control of a biomimetic hexapedal walker, 2008).

Figure 2.5

Pneumatic Based Robot (Wait & Goldfarb, 2014)

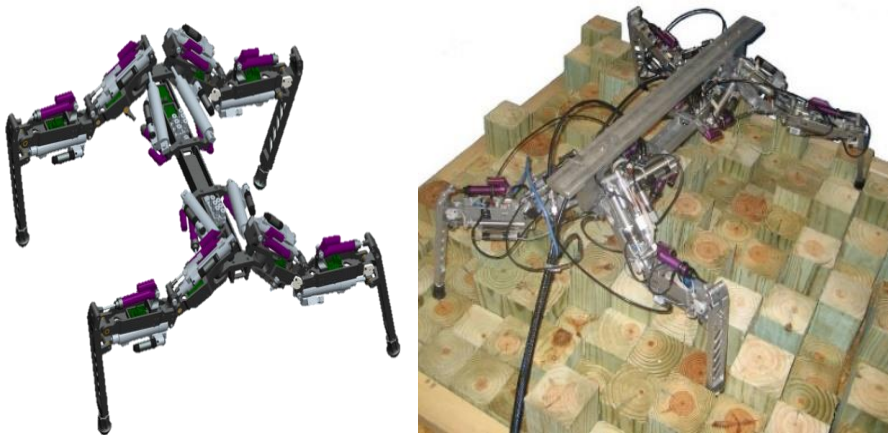

TITAN XIII (Kitano, 2016) an optimized design of TITAN VIII (Arikawa & Hirose, 1996), used DC brushless motors with wire driven mechanism to drive the lower link (shank) of the robot.

Developers proposed to reduce the cost of transport by increasing walking velocity as well as they proposed to reduce the energy of gravitational support. Moreover, Researchers compared the different driven techniques for leg i.e. parallel-type and right angle-type wired driven mechanism and compared the results of many other features as well.

Figure 2.6

TITAN XIII Robot with Two Configurations of Wire Driven Mechanism (Kitano, 2016)

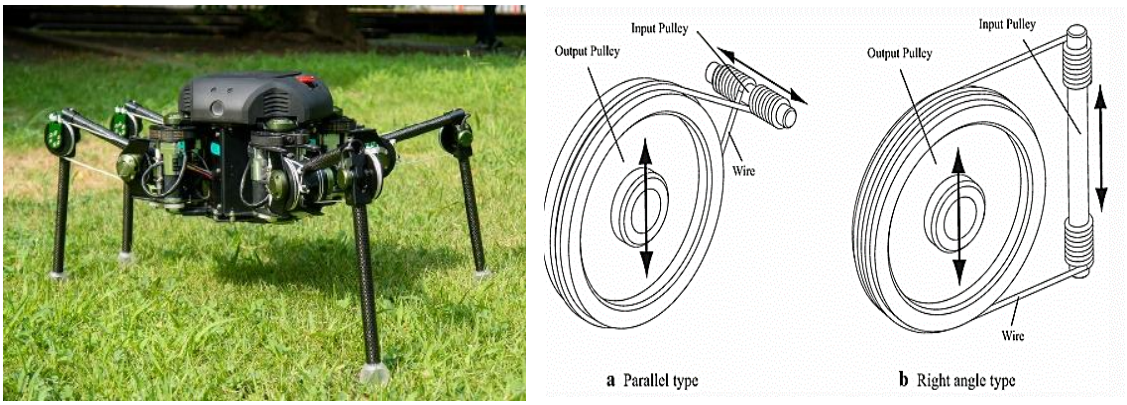

2.1.2 Mammal-Type Quadruped Robot

Robotic Challenges and advanced research have motivated many research groups to put their efforts in developing very robust and efficient quadruped robot and urged them to developed very advance control.

ANYmal (Hutter, et al., 2016) robot introduced by ETH for autonomous navigation and to climb on obstacles in challenging and uneven environment. This robot was used in two different challenges named as ARGOS inspection challenge as well as the NCCR challenge for Search and Rescue. Quadrupedal robot had 4 carbon legs equipped with contact sensors at bottom of each leg. The power sources, controller, network system, navigation sensors and power distribution circuits were integrated in a single unit called main body. They used WiFi link to access the intel NUC PCs installed in ANYmal for any operation. For thermal stability, all components were coupled with main body which behaved as heat sink. At the back side, small HMI display were installed to power up individual computers and sensors of the robot.

Figure 2.7

ANYmal Robot with OFF Mode Configuration (Hutter, et al., 2016)

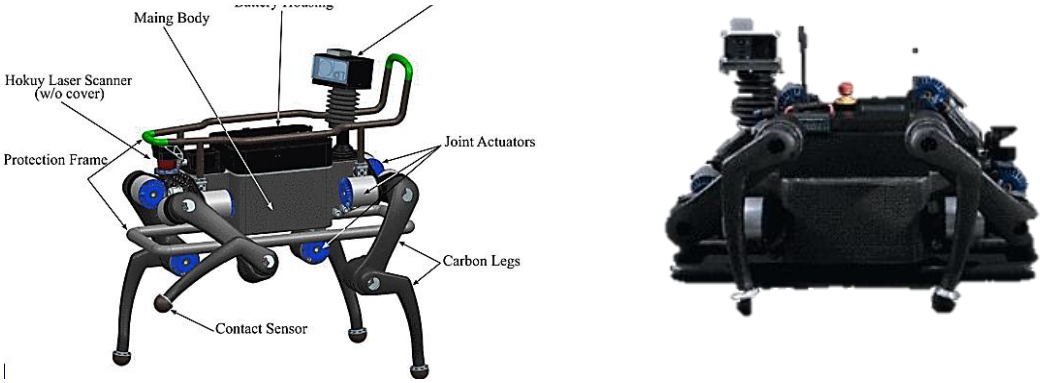

For the software side, three intel PCs shared the individual tasks i.e. navigation, motion, and inspection. In addition, to integrate all process, Robotic Operating System (ROS) on linux were used to transfer of data.

Stanford Doggo (Kau, Schultz, Ferrante, & Slade, 2019) fabricated to present the quasi-direct-drive methodology, adopted by the research team to improve the vertical speed, and jumping alertness. Moreover, they succeeded in getting 22% improve performance than the preceding best quadrupedal robot (Haldane, Yim, & Fearing, 2017).

The proposed mechanical designed had 3:1 belt drive system to transmit power from actuator to driven shafts as well as the wireless communication was established by XBee module. The reason to choose belt drive over gear was to reduce reflected inertia and weight of the system. Moreover, the proposed model of leg had less chances of singularity conditions.

Figure 2.8

Stanford Doggo Robot with Quasi-Drive Direct Mechanism (Kau, Schultz, Ferrante, & Slade, 2019)

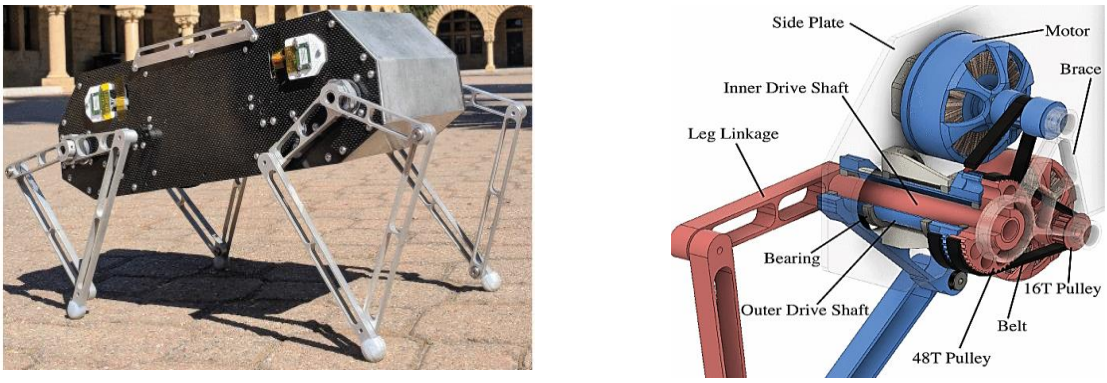

Cheetah 3 (Nguyen, Powell, Katz, Carlo, & Kim, 2019) robot built by MIT research group to introduce the advance features and enhance the jumping agility in previous built Cheetah1 and 2 robots. Before the development of cheetah 3, another research group presented the optimized jumping in a robot with single leg and that system was very small with link length of about 12cm (Ding & Park, 2017). Cheetah 3 with robust behavior towards takeoff and landing from a height of 0.76m had ability to stabilize the body orientation and position of the robot as well as trajectory optimization. This platform used high torque customized electric actuators with planetary gear reduction along with optimized control of gravitational reaction forces through concept of proprioception without using force and torque sensors.

Figure 2.9

Cheetah 3 Robot Developed at MIT having Planetary Gear Reduction (Nguyen, Powell, Katz, Carlo, & Kim, 2019)

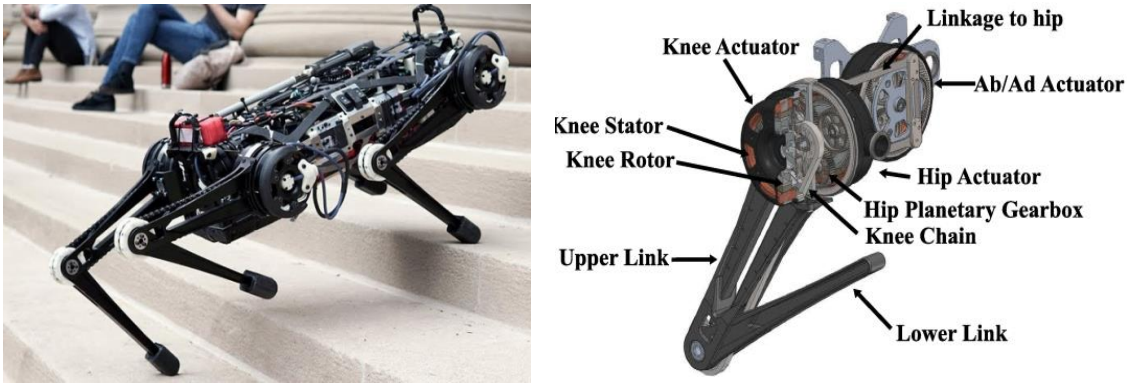

Artificial Digitigrade for Natural Environments AiDIN-VI (Lee, et al., 2020) robot developed in the lab of Korea with controllable force which consolidate speed of robot, efficiency, and mobility to support services of real-world. The robot equipped with onboard computers for vision and motion control along with network router, power source (batteries), and remote controller for emergency stop in both manual and auto mode. Moreover, torque sensor used in joints for angles were capacitive type and developed robot has ability to control ±70Nm joint torque as well as it can walk with the speed of about 1.2 m/s. In addition, under loaded conditions, it has cost of transport 1.18 and 1.15 with minimum speed of 1.0 m/s. Developed robot was tested in the different rough and tough terrain and experimentally succeeded to get good performance.

Figure 2.10

AiDIN-VI Quadruped Developed by Korean Researchers (Lee, et al., 2020)

2.2 Balancing Controls of Legged-Robots

In this section, balancing theories adopted in literature would be discussed. Balancing controls are the most trending research in legged robot along with optimized functionalities in rough terrain.

In static balancing for quadruped robot, first thing to consider is center of mass (COM) which should along the gravitational acceleration within closed polygon. Moreover, to achieved static equilibrium, COM requirements should be satisfied (Lakatos, et al., A Coordinate-based Approach for Static Balancing and Walking Control of Compliantly Actuated Legged Robots, 2019)

The proposed walking algorithm (Lakatos, et al., A Coordinate-based Approach for Static Balancing and Walking Control of Compliantly Actuated Legged Robots, 2019) for balancing did not used the map and absolute position of the system but measured the orientation of legs configuration with respect to gravity and base respectively. Algorithm followed by the given below sequence.

1. Adjust the center of mass in supporting polygon to move one leg for next step.
2. Drop off the foot and move until contact detected.
3. Recapture contact if not all legs are in contact with ground.
4. Adjust the foot position to be move for next step according to terrain height.
5. Place foot on surface which has been dislocated.

Pneumatic actuated legged robot has produced the stable walking by using joint control units along with trajectories. The proposed strategy considers keeping the center of mass in polygon developed by legs in stance phase as well as to sustain the kinematic consistency in between legs. As the robot move by displacing any leg, the polygon always move accordingly. Hence to maintain the balance, controller required to keep the center of mass in the polygon (Wait & Goldfarb, 2014).

Figure 2.11

ANYmal Robot Control Algorithm (Hutter, et al., 2016)

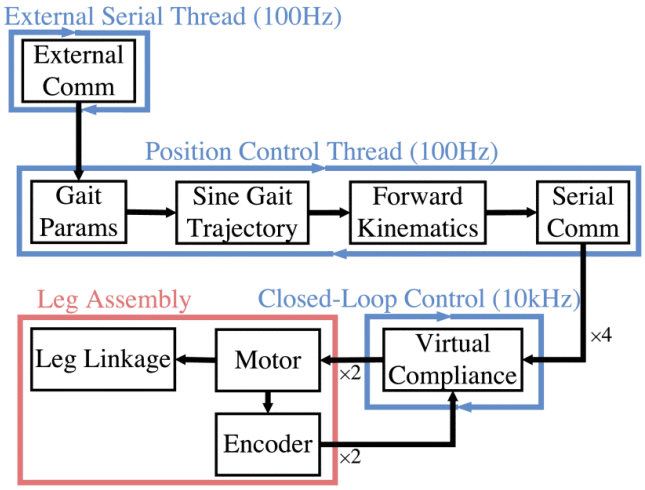

ANYmal robot used the cascaded joint position, torque, and compliance control by contemplate the motor as torque supplier. Torque controller basically consisted of three blocks called as PID controller, feedback friction compensation along with feed forward term. Moreover, torque controller measured the required torque and decided required current to produce that torque as well as the difference in gear and joint position used to measure the spring deflection (Hutter, et al., 2016).

Stanford Doggo with a unique design with minimum actuations considered the different parameters including time for traversing each sinusoidal segment by leg as well as the leg compliance used to develop gait trajectories. Then these required postures of gait converted to required joint angles in terms of forward kinematics. PD control used by motor controllers to produce required output torques and desired joint angles (Kau, Schultz, Ferrante, & Slade, 2019).

Figure 2.12

Stanford Doggo Robot Control Algorithm (Kau, Schultz, Ferrante, & Slade, 2019)

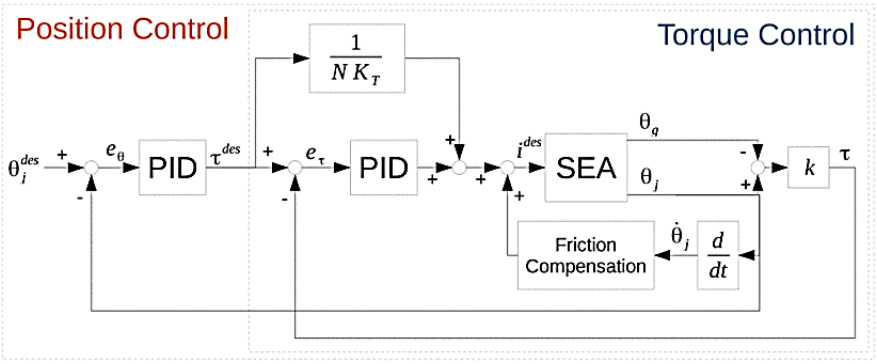

CHAPTER 3
METHODOLOGY

3.1 Robot Selection Parameters:

Most challenging job in quadruped robot is to design an optimized mechanical structure with least singularity conditions. Basic aim is of this research is to develop a four-legged robot which can walk and stand in up right condition by applying balancing control. There are two different types of quadruped as shown below i.e. Sprawling and Mammal like legged robots.

While walking of robot, center of mass changes, hence a robust control is needed to maintain its balance. Moreover, for trotting, we need to develop the dynamic control for only two stance legs for balancing as well as the control should be robust against environmental disturbances. The proposed design concepts are given below with same 12 degree of freedoms having 3 DOF on each leg actuated by high torque DC motors.

Table 3.1

Hardware Specifications of Quadruped Robot

Parameters	**Specification values**
Hardware Material	Iron and Steel
Hip Joint Material	Aluminum
Length	400mm
Width	280mm
Height	388.57mm
Weight	10.25 kg
Degree of Freedom	12
DC Motor Power	18Wx8, 25Wx4

3.2 Mechanical Design of Quadruped Robot.

Mechanical design has been developed on software named “SolidWorks”. CAD of each individual part with dimensions is attached in appendix.

Figure 3.1

Side View of Quadruped Robot

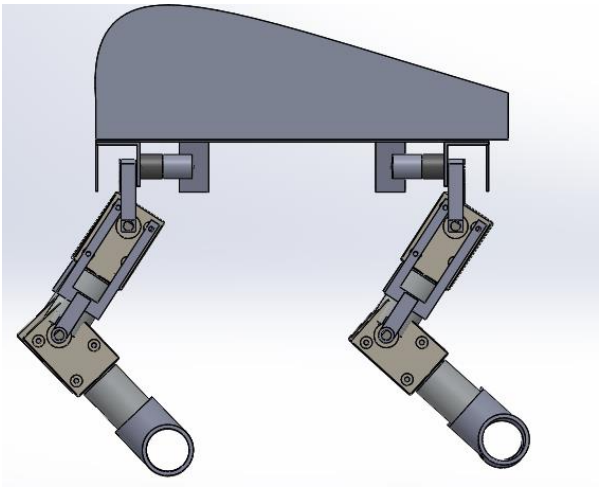

The first figure represents the side view of quadruped robot and the second figure presents the 3D view of robot.

Figure 3.2

3D Model of Quadruped Robot developed on Solidworks

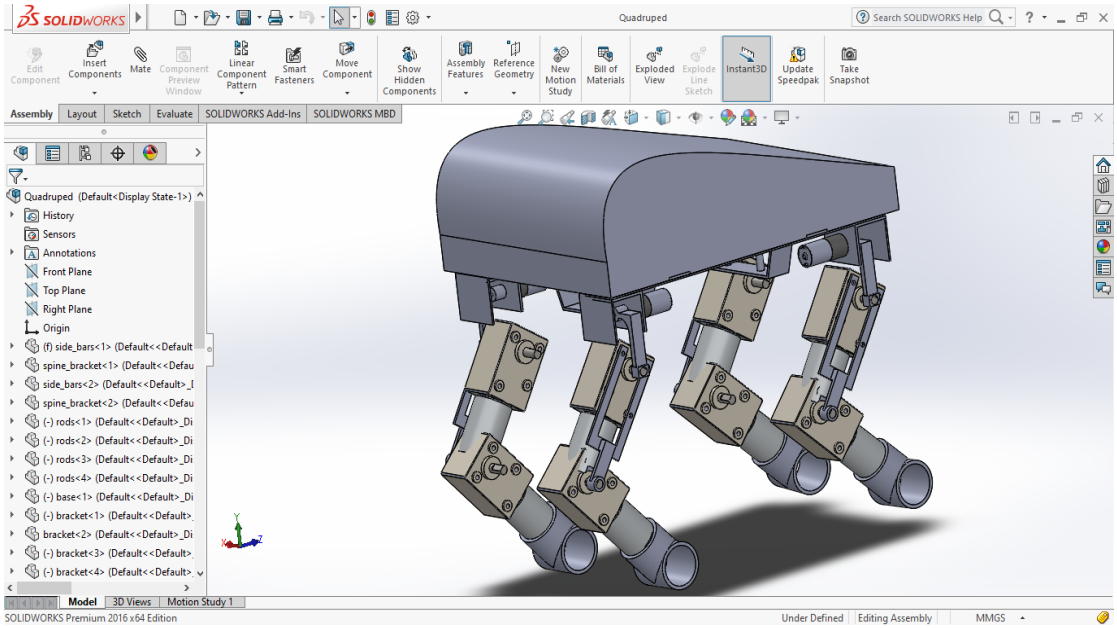

Figure 3.3

Hardware of Quadruped Robot Developed at AIT

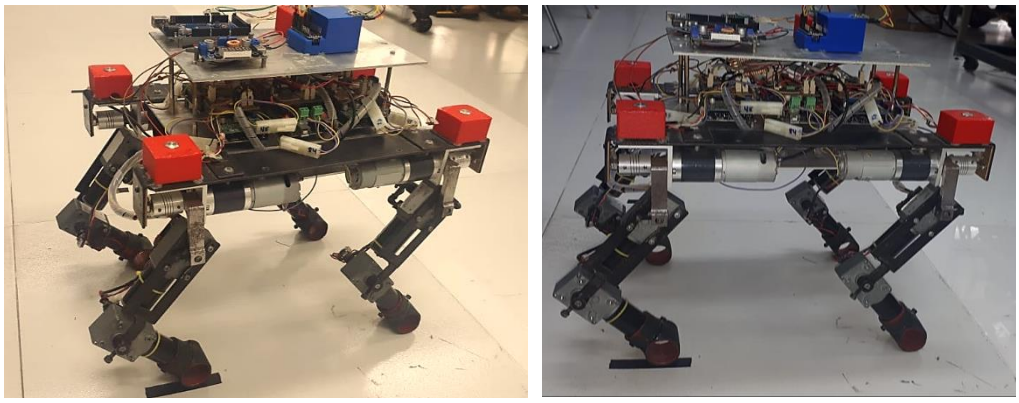

3.3 Robot Kinematics

Quadruped robot has four legs, and each has same configuration with 3 degree of freedoms. Hence, to determine the kinematics, we considered one leg for DH Parameters.

Table 3.2

DH Parameters of Robot

Parameter	Link 1	Link 2	Link 3
l_i	l_1	l_2	l_3
α_i	$\pi/2$	0	0
d_i	0	0	0
θ_i	θ_1	θ_2	θ_3

Figure 3.4

DH Parameter of Quadruped Robot

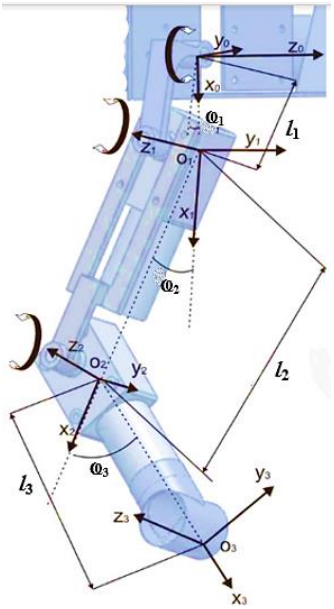

Homogenous transformation matrices for single leg of the robot are given below.

$$A_0^1 = \begin{pmatrix} cos\,\theta_1 & 0 & sin\,\theta_1 & l_1\,cos\,\theta_1 \\ sin\,\theta_1 & 0 & -cos\,\theta_1 & l_1\,sin\,\theta_1 \\ 0 & 1 & 0 & 0 \\ 0 & 0 & 0 & 1 \end{pmatrix}$$

$$A_1^2 = \begin{pmatrix} cos\,\theta_2 & -sin\,\theta_2 & 0 & l_2\,cos\,\theta_2 \\ sin\,\theta_2 & cos\,\theta_2 & 0 & l_2\,sin\,\theta_2 \\ 0 & 0 & 1 & 0 \\ 0 & 0 & 0 & 1 \end{pmatrix}$$

$$A_2^3 = \begin{pmatrix} cos\,\theta_3 & -sin\,\theta_3 & 0 & l_3\,cos\,\theta_3 \\ sin\,\theta_3 & cos\,\theta_3 & 0 & l_3\,sin\,\theta_3 \\ 0 & 0 & 1 & 0 \\ 0 & 0 & 0 & 1 \end{pmatrix}$$

$$A_0^3 = A_0^1 A_1^2 A_2^3 = \begin{pmatrix} R_{3x3} & p_{3x1} \\ 0_{1x3} & 1 \end{pmatrix}$$

$$= \begin{pmatrix} cos\,\theta_1\,cos(\theta_2+\theta_3) & -sin(\theta_2+\theta_3)\,cos\,\theta_1 & sin\,\theta_1 & cos\,\theta_1\,(l_3\,cos(\theta_2+\theta_3)+l_2\,cos\,\theta_2+l_1) \\ sin\,\theta_1\,cos(\theta_2+\theta_3) & -sin(\theta_2+\theta_3)\,cos\,\theta_1 & -cos\,\theta_1 & sin\,\theta_1\,(l_3\,cos(\theta_2+\theta_3)+l_2\,cos\,\theta_2+l_1) \\ sin(\theta_2+\theta_3) & cos(\theta_2+\theta_3) & 0 & l_3\,sin(\theta_2+\theta_3)+l_2\,sin\,\theta_2 \\ 0 & 0 & 0 & 1 \end{pmatrix}$$

Here, $p = \begin{bmatrix} x \\ y \\ z \end{bmatrix}$ is the end effector position vector. Hence x, y and z coordinates of bottom tip of the leg are given below.

$$x = cos\,\theta_1\,(l_3\,cos(\theta_2+\theta_3)+l_2\,cos\,\theta_2+l_1) \quad (3.1)$$

$$y = sin\,\theta_1\,(l_3\,cos(\theta_2+\theta_3)+l_2\,cos\,\theta_2+l_1) \quad (3.2)$$

$$z = l_3\,sin(\theta_2+\theta_3)+l_2\,sin\,\theta_2 \quad (3.3)$$

To determine the joint angles for the end effector position of the leg, we need to calculate the inverse kinematics using the above three equations.

$$x\,sin(\theta_1) = y\,cos(\theta_1) \quad (3.4)$$

$$\frac{sin\,\theta_1}{cos\,\theta_1} = \frac{y}{x}$$

$$tan\,\theta_1 = \frac{y}{x}$$

$$\mathbb{Q}_1 = \tan^{-1}\frac{y}{x} \tag{3.5}$$

Similarly, for the second angle $\mathbb{Q}_2$, we used equation (3.1) and (3.2) to find the following equation.

$$cos(\mathbb{Q}_2 + \mathbb{Q}_3) = \frac{x\,cos\,\mathbb{Q}_1 + y\,sin\,\mathbb{Q}_1 - l_2\,cos\,\mathbb{Q}_2 - l_1}{l_3} \tag{3.6}$$

From equation (3.3)

$$sin(\mathbb{Q}_2 + \mathbb{Q}_3) = \frac{z - l_2\,sin\,\mathbb{Q}_2}{l_3} \tag{3.7}$$

Substitute the values of $cos(\mathbb{Q}_2 + \mathbb{Q}_3)$ and $sin(\mathbb{Q}_2 + \mathbb{Q}_3)$ into general equation given below.

$$sin^2\vartheta + cos^2\vartheta = 1 \tag{3.8}$$

After re-arranging and simplifying, we got the equations in terms of substitutes A, B and C respectively.

$$-z.sin\mathbb{Q}_2 + l_1 - (x\,cos\,\mathbb{Q}_1 + y\,sin\,\mathbb{Q}_1).cos\mathbb{Q}_2$$

$$= \frac{2l_1(x\,cos\,\mathbb{Q}_1 + y\,sin\,\mathbb{Q}_1) + l_3^2 - l_2^2 - l_1^2 - z^2 - (x\,cos\,\mathbb{Q}_1 + y\,sin\,\mathbb{Q}_1)^2}{2l_2} \tag{3.9}$$

$$A = -z$$

$$B = l_1 - (x\,cos\,\mathbb{Q}_1 + y\,sin\,\mathbb{Q}_1)$$

$$C = \frac{2l_1(x\,cos\,\mathbb{Q}_1 + y\,sin\,\mathbb{Q}_1) + l_3^2 - l_2^2 - l_1^2 - z^2 - (x\,cos\,\mathbb{Q}_1 + y\,sin\,\mathbb{Q}_1)^2}{2l_2}$$

Hence equation (3.9) becomes.

$$A.sin\,\mathbb{Q}_2 + B.cos\,\mathbb{Q}_2 = C \tag{3.10}$$

As we know,

$$A = r\cos\emptyset$$

$$B = r\sin\emptyset$$

$$\emptyset = \tan^{-1}\left[\frac{B}{A}\right]$$

$$r = \pm\sqrt{A^2 + B^2}$$

Hence equation (3.10) can be rewritten as

$$cos\,\emptyset\,sin\,\mathbb{Q}_2 + sin\,\emptyset\,cos\,\mathbb{Q}_2 = \frac{C}{r}$$

$$sin(\emptyset + \mathbb{Q}_2) = \frac{C}{r}$$

From equation (3.8)

$$cos(\emptyset + \mathbb{Q}_2) = \pm\sqrt{1 - sin^2(\emptyset + \mathbb{Q}_2)} = \frac{\pm\sqrt{r^2 - C^2}}{r}$$

$$tan(\emptyset + \mathbb{Q}_2) = \frac{C}{\pm\sqrt{r^2 - C^2}}$$

After re-arranging the above equation and substitute the value of $\emptyset$, we got the following result.

$$\mathbb{Q}_2 = -\tan^{-1}\left(\frac{B}{A}\right) + \tan^{-1}\left(\frac{C}{\pm\sqrt{r^2 - C^2}}\right)$$

From equation (3.6) and (3.7)

$$\mathbb{Q}_3 = \tan^{-1}\left(\frac{z - l_2\,sin\,\mathbb{Q}_2}{x\,cos\,\mathbb{Q}_1 + y\,sin\,\mathbb{Q}_1 - l_2\,cos\,\mathbb{Q}_2 - l_1}\right) - \mathbb{Q}_2$$

Hence, the joint angles for each leg can be determined by the end effector position coordinates of leg.

$$\mathbb{Q}_1 = \tan^{-1}\frac{y}{x}$$

$$\mathbb{Q}_2 = -\tan^{-1}\left(\frac{l_1 - (x\,cos\,\mathbb{Q}_1 + y\,sin\,\mathbb{Q}_1)}{-Z}\right) + \tan^{-1}\left(\frac{C}{\pm\sqrt{r^2 - C^2}}\right)$$

$$\mathbb{Q}_3 = \tan^{-1}\left(\frac{z - l_2\,sin\,\mathbb{Q}_2}{x\,cos\,\mathbb{Q}_1 + y\,sin\,\mathbb{Q}_1 - l_2\,cos\,\mathbb{Q}_2 - l_1}\right) - \mathbb{Q}_2$$

3.4 Electrical Concept

Quadruped robot used the two controller levels i.e., high-level, and low-level controller. In low level controller, speed, and position control of 12 motors is applied alongside balancing control, gait tracking and retrieval against disturbances control is implemented in high level controller. Whole system get power from power distribution circuit having source of DC 12 Volts and the actuators voltage can vary between 9 to

12 Volts. Moreover, 6 axes inertial measurement unit (IMU 6050 having 3 axes gyroscope and 3 axes accelerometer) is being used in robot for balancing. The low-level controller communicates with high-level controller using serial communication, while the whole system communicates using Bluetooth module for getting commands from user to tune the system. The entire architecture of robot is presented in figure 3.8.

Table 3.3

Summary of Electronic Components

Electronic Devices	**Purpose of Use**
Arduino AT Mega 2560	Balancing Control and Gait Generation
Arduino DUE	Control against Environmental Impedances
Arduino UNO	For Motor shields to actuate motors
Motor Driving shields	For DC Motors Actuations
IMU 6050	Gyroscope and Accelerometer Unit
Bluetooth HC06	Wireless communication
Joystick Controller	For robot movement commands

Each Arduino UNO controller with motor shields used for controlling the position and velocity of the 2 DC motors. For 12 degree of freedom robot, 6 Arduino UNO boards used with motor shields. Each Arduino board receive command through serial communication from high level controller Arduino Mega 2560 according to gait pattern along with balancing instructions and actuate the motors accordingly.

Figure 3.5

Arduino UNO R3

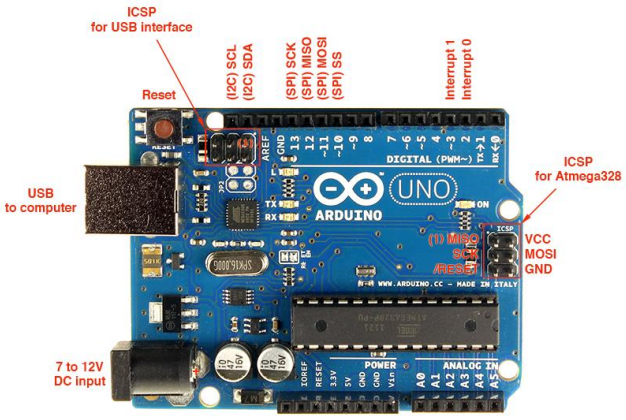

Figure 3.6

Polulu Driver with Arduino

Arduino UNO has 16 MHz crystal along with ATMega328 chip, 6 analog Input pins and 14 digital I/O's along with 6 PWM pins. Moreover, motor shield of Polulu has used with Arduino to control the direction of DC motor. It has VNH2SP30 chip with high voltage and current ratings along with polarity protection. This driver communicates with Arduino through UART protocol and can control 2 DC motors simultaneously. It includes logic control unit, linear current limiter, over temperature protection and fault detection.

Figure 3.7

Real Time Structure of Polulu Driver with Arduino

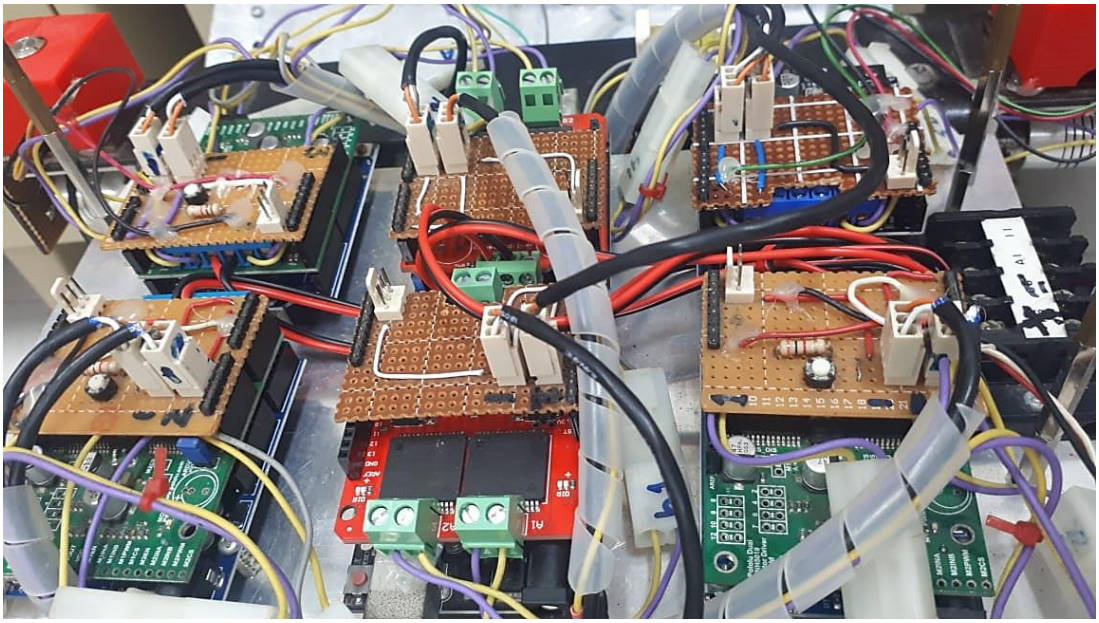

Systematic structure of all motors along with VNH2SP30 chip drivers is presented in the figure 3.6.

High-level controller consists of Arduino Mega 2560 and Arduino Nano for gait pattern generation along with balancing and control against external lateral forces, respectively. Arduino Mega has 16 MHz crystal and ATMega 2560 controller chip as well as it has 54 digital I/O's, 16 analog input pins and 4 UART (serial communication ports).

Figure 3.8

Arduino AT Mega 2560

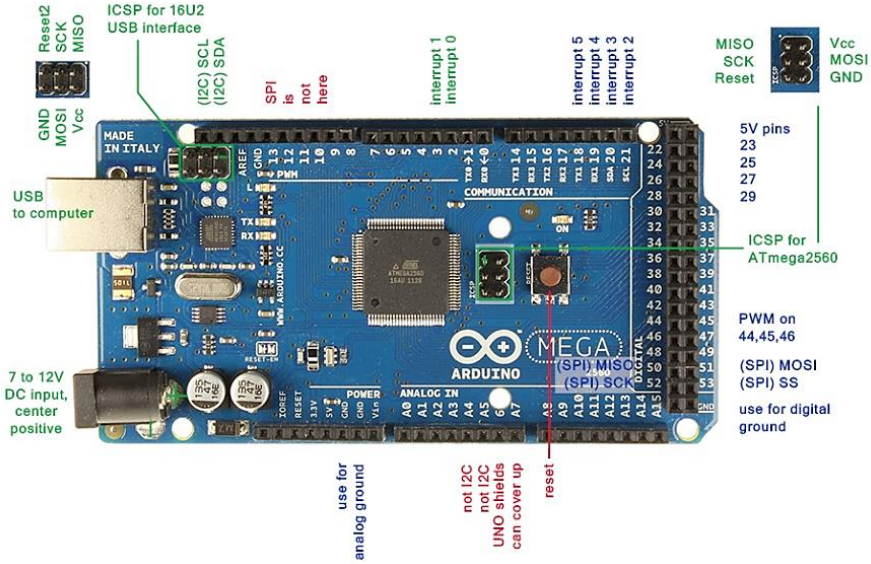

Figure 3.9

Detailed Architecture of Quadruped Robot

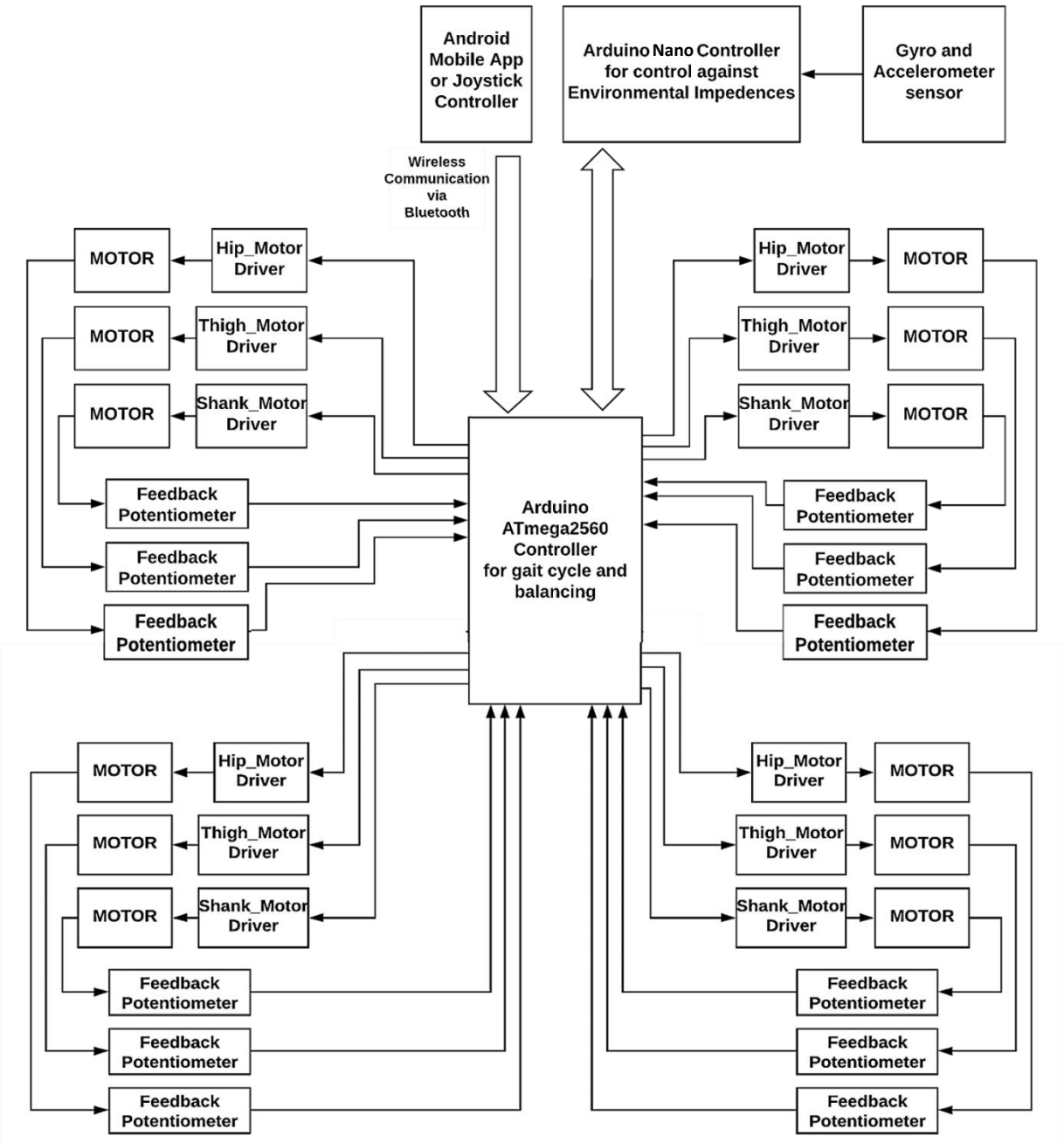

3.4.1 Power Distribution System

Power distribution system has 2 sub-systems, the 12 Volts for powering the DC motors and 9 volts for operating the electronic circuitry including Bluetooth module, IMU sensor and Arduino boards of high-level controller. Detail power distribution system is shown in figure below.

Figure 3.10

Power Distribution Architecture

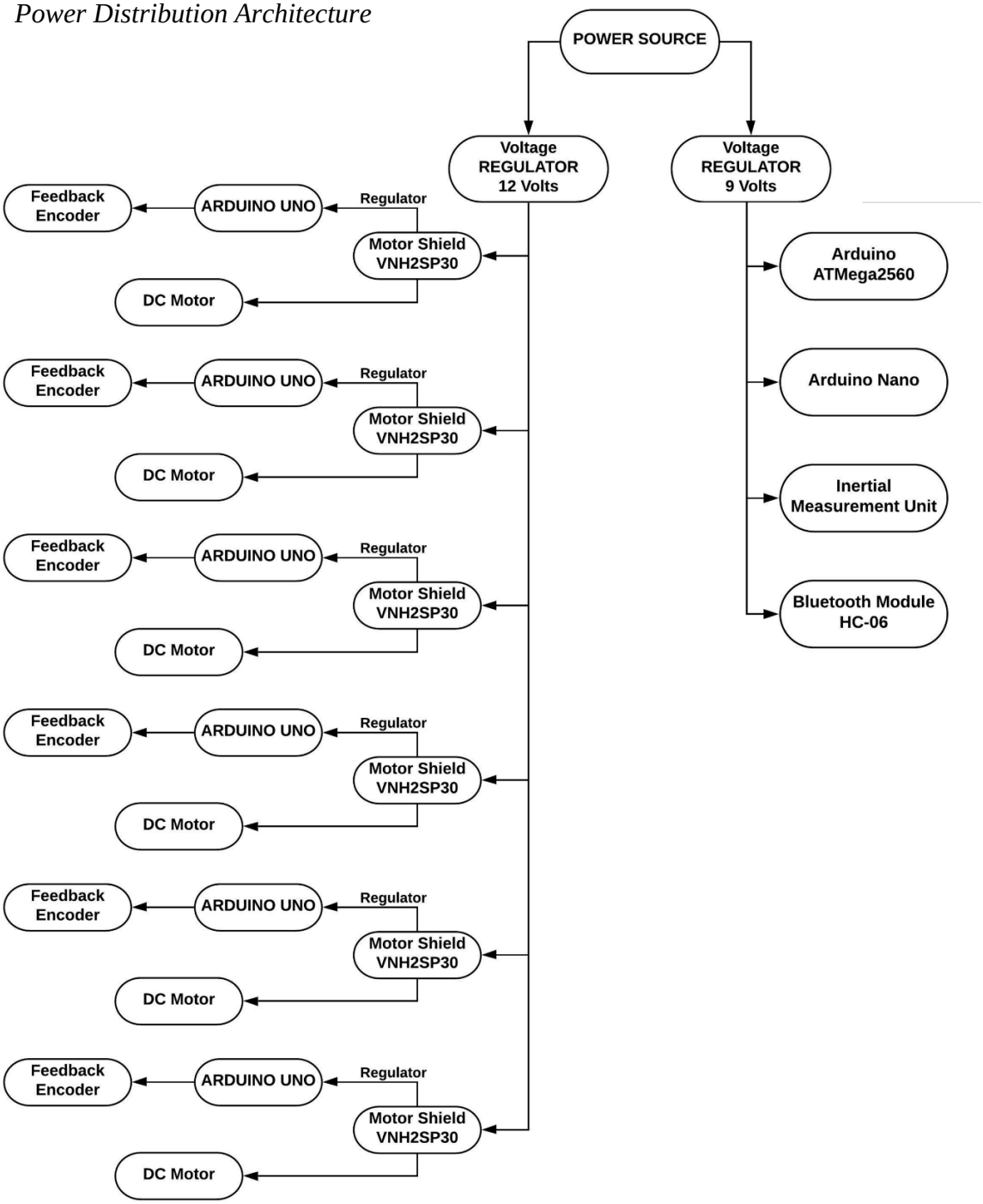

Figure 3.11

Power Distribution System of Robot

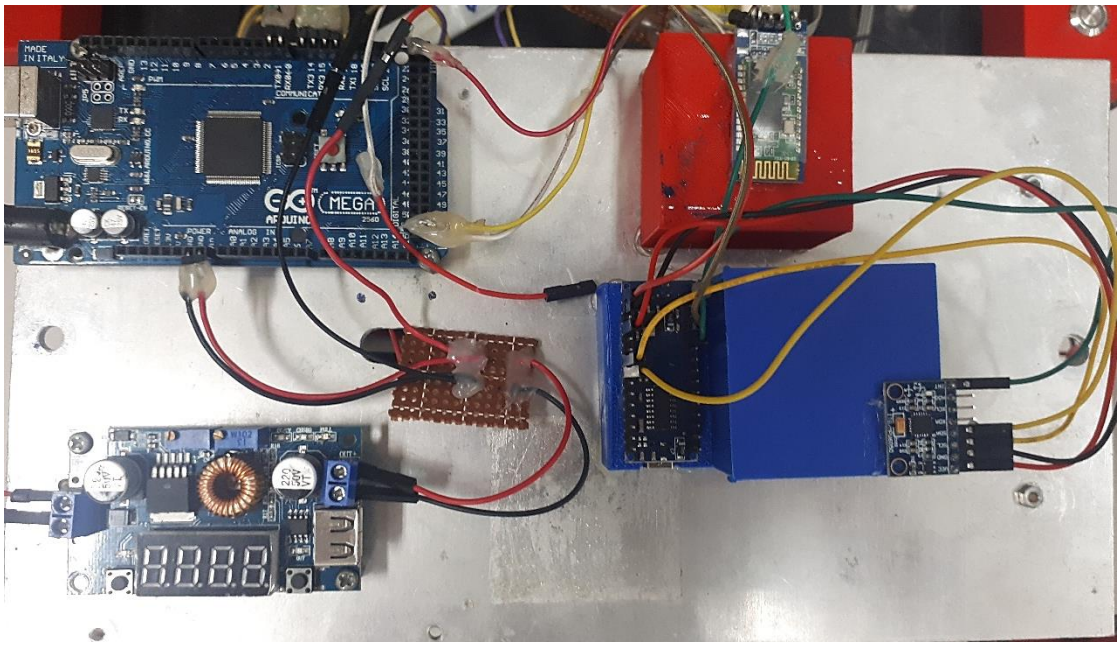

Inertial measurement unit is a sensor of model MPU6050 consists of 3 axes gyroscope (IDG500) which gives roll, pitch, and yaw to control the orientation of the robot for balancing and it contains 3 axes accelerometer (ADXL345) to determine the acceleration produce by external forces or disturbances. Communication take place through I2C protocol between Arduino and measurement unit. Furthermore, this sensor produces several raw values due to real time environment noises. To minimize the noise, Kalman filter is used for getting the values of the IMU.

Figure 3.12

Inertial Measurement Unit (MPU 6050)

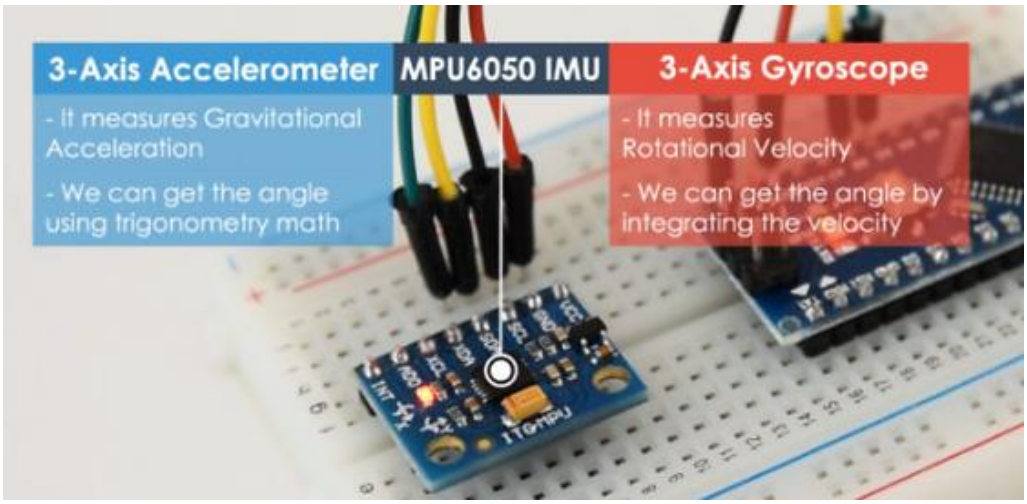

3.5 Kalman Filter Fusion

To estimate the states of progression by minimizing the mean squared errors, Kalman filter is used. Basic aim of Kalman filter is to reduce the effect of environmental noises as well as undesired signals.

Kalman filter has 2 stages in a cycle i.e., prediction, and correction.

1. In prediction stage, filter predicts the error covariance and state estimate of the system.

$$\bar{\hat{x}}_k = A\hat{x}_{k-1} + Bu_{k-1} \quad (3.14)$$

$$\bar{P}_k = AP_{k-1}A^T + Q \quad (3.15)$$

Equation (3.14) determines the predicted state estimate, *x* is the system state, A is dynamic matrix, B and *u* are control matrix and control input, respectively. Equation (3.15) determines the error between actual state variable and the estimate of x, called as predicted error covariance, P and Q are the matrices of covariance and process disturbance covariance, respectively.

Figure 3.13

Two Step Estimation Filter

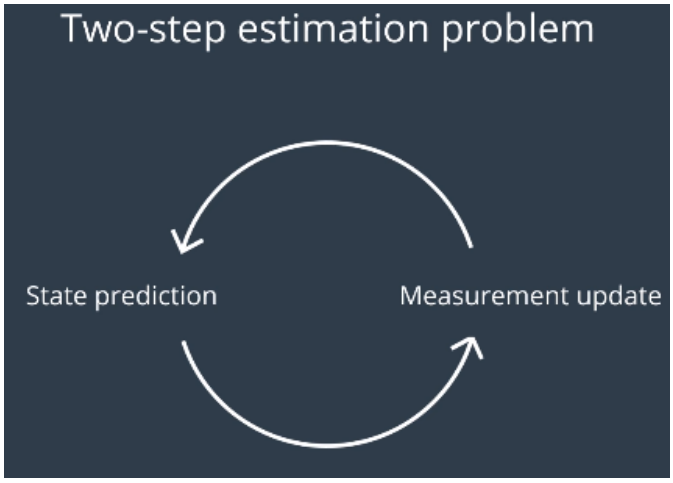

2. In update step, the filter gets response from the sensor, and update the estimated states with the feedback of sensor.

$$K_k = \bar{P}_k H^T (H \bar{P}_k H^T + R)^{-1} \quad (3.16)$$

$$\hat{x}_k = \bar{\hat{x}}_k + K_k (z_k + H \bar{\hat{x}}_k) \quad (3.17)$$

$$P_k = (1 - K_k H)\,\bar{P}_k \qquad (3.18)$$

Equation (3.16) determines the gain to minimize the error covariance, Kalman gain value will decrease if the difference between predicted value and measured feedback value decreases. Matrices H and R are the measurement matrix and measurement disturbance covariance matrix, respectively. Equation (3.17) determines the measurement update estimate state and (3.18) determines the updated error covariance.

Figure 3.14

Kalman Filter Loop Structure

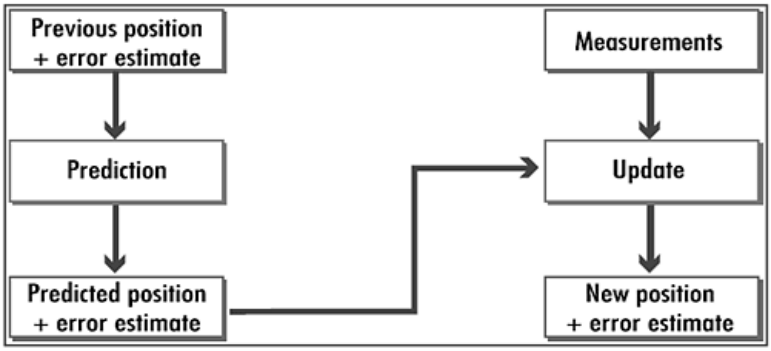

In the quadruped robot, two state Kalman filter has used. Because of fusion of two sensors i.e., accelerometer and gyroscope sensor, and the response time is good enough to control the orientation and behavior against external lateral forces. Figure (3.14) shows the actual raw signal and filtered signal of the accelerometer sensor.

Figure 3.15

Comparison of Raw and Kalman Fusion Output of Accelerometer

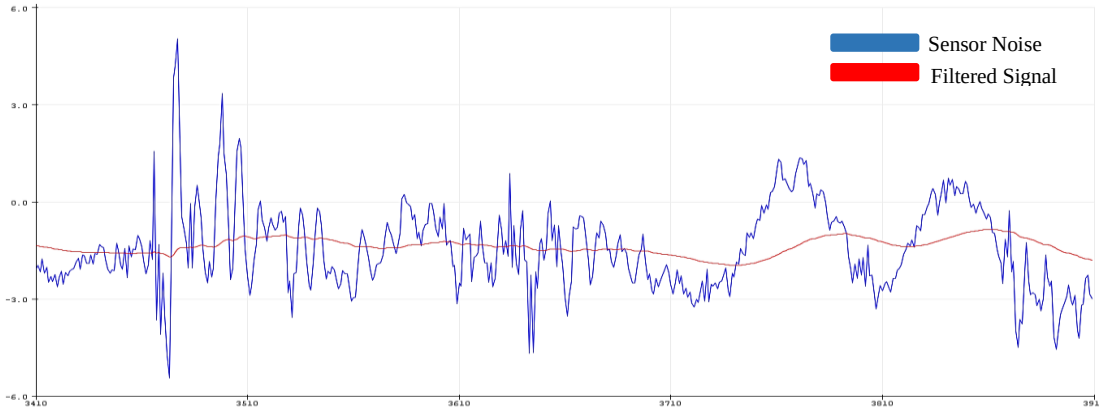

Figure 3.16

Raw Values of Gyroscope Sensor

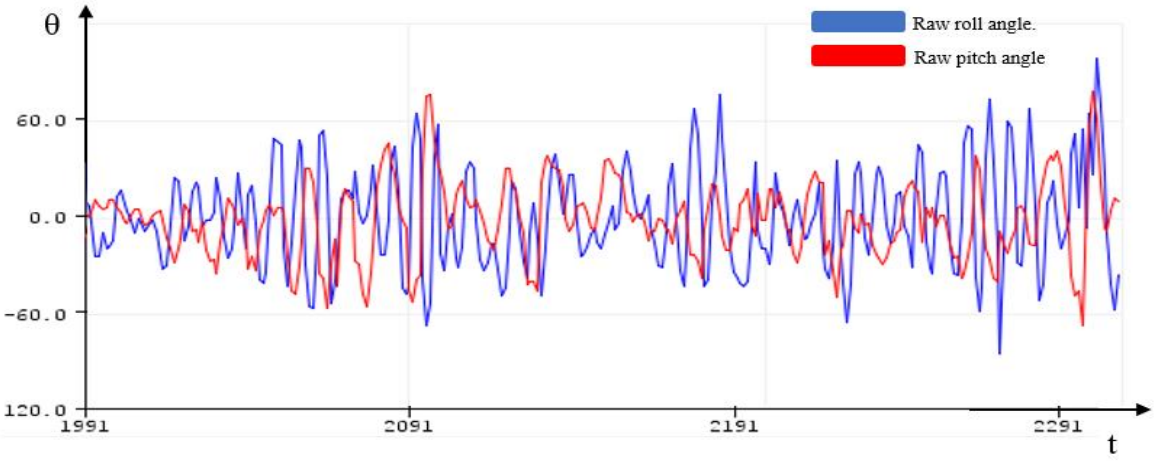

Figure 3.17

Kalman Fusion Output of Gyroscope Sensor

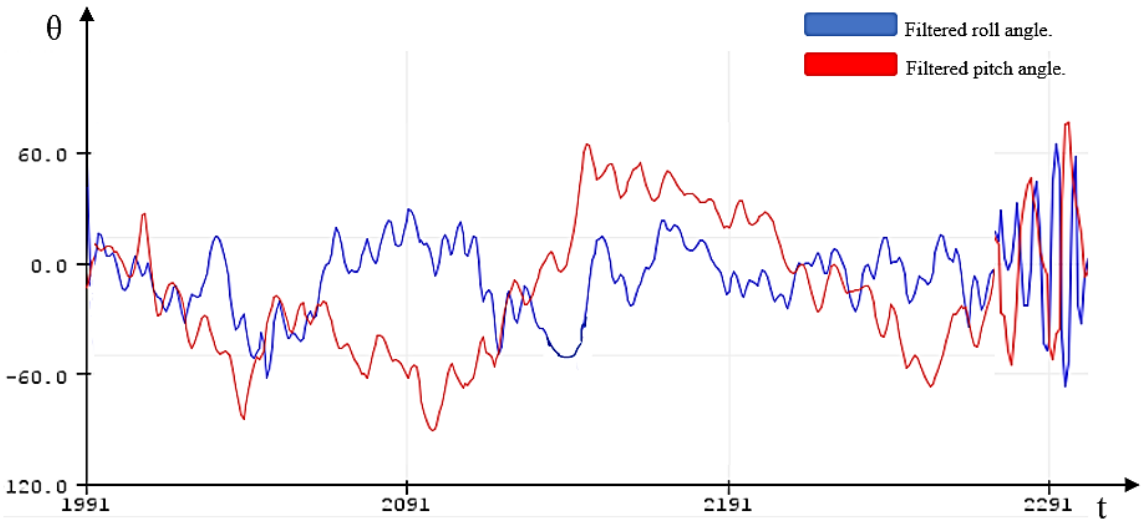

CHAPTER 4
CONTROL OF QUADRUPED ROBOT

4.1 Control Architecture of Quadruped Robot

Control architecture of robot consists of two controller levels i.e., high-level, and low-level controller. The high-level controller comprises of gait generator, that provides walking trajectory to move the robot in forward/backward directions. Zero Moment Point (ZMP) based balancing control develop a free gait to balance the body of the robot using the roll, pitch and yaw angles provided by the measurement unit. Moreover, Retrieval against disturbances control determines the sideway(lateral) disturbances using accelerometer and combined with gait generator provides a retrieving footstep position to avoid the robot from fall.

Figure 4.1

Control Architecture of Quadruped Robot

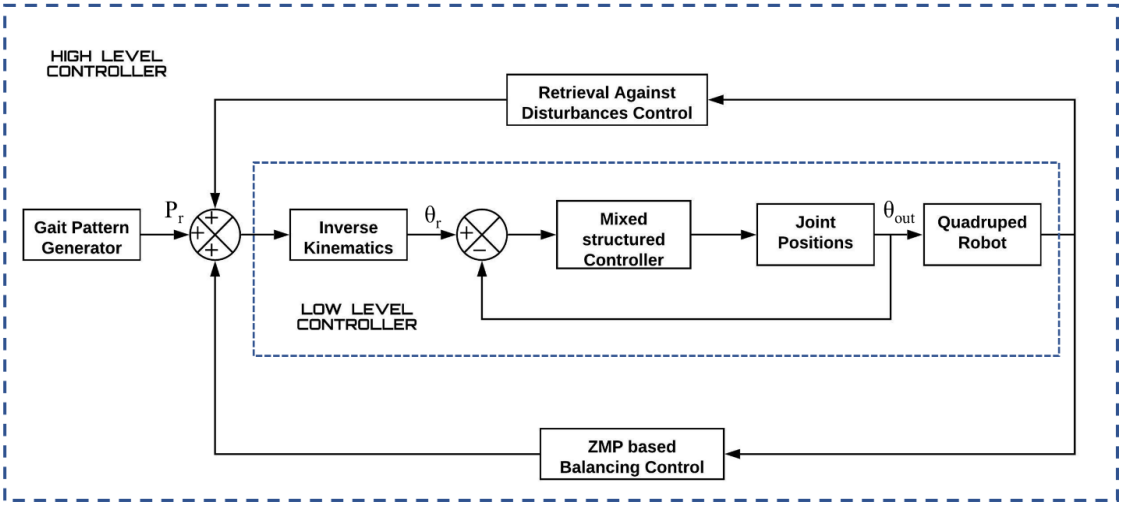

Low level controller is the basic block of the controller as it generates the joint angles for each leg using inverse kinematics of the robot. All the controllers combined with gait generator provides the position of the end effector of each leg to the low-level controller. It determines the joint angles of each leg using proposed mixed H2 / H∞ structured controller. All the control input data is generated by the 6 axes inertial measurement unit (IMU), which has 3 axes gyro and 3 axes accelerometer sensor. The terms used to present the control architecture involves P_r for required position of end effector, θ_r for required joint angles and θ_{out} for output joint angles.

4.2 Balancing Control of Quadruped Robot

Quadruped robot can be considered as two biped robots carrying a mass between them as shown in figure 4.2. During trotting, quadruped robot endorsed by two legs in diagonal positions, because two diagonal legs remain in stance phase and two remain in swing phase simultaneously. Hence, center of mass shifts horizontally in longitudinal direction and make the robot unbalanced. To keep the robot balanced, balancing control is implemented, and quadruped robot is modeled as simplified model of biped robot during trotting. Moreover, center of mass can is considered as point mass of two-legged robot.

Figure 4.2

Biped Robot Model Equivalence of Quadruped Robot

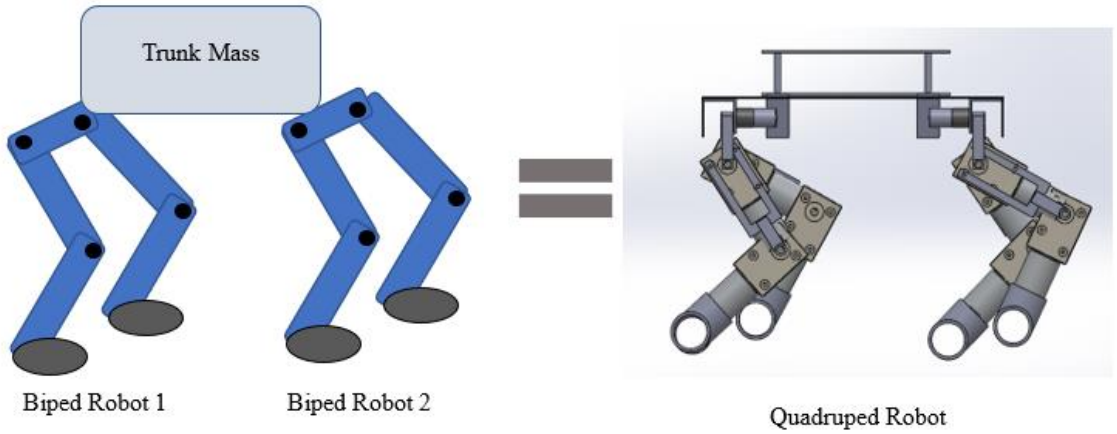

Many researchers proposed different balancing technique, one of those most used is linear inverted pendulum for two-legged robots. Hence, this quadruped robot has adopted the linear inverted pendulum model having a point mass using Zero Moment Point approach.

Zero Moment Point (ZMP) is the theory used for the dynamic stability of legged robots. ZMP is the point on the ground where moment is not produced by the dynamic reaction force in horizontal direction. Body remains balanced while keeping the ZMP in the supporting line or polygon made by diagonal legs. In our case, supporting stripe is developed by the surface area of the foot, mentioned in the figure 4.3. and the supporting stripe is shown in figure 4.4.

Figure 4.3

Surface Area of Foot in Contact with Ground

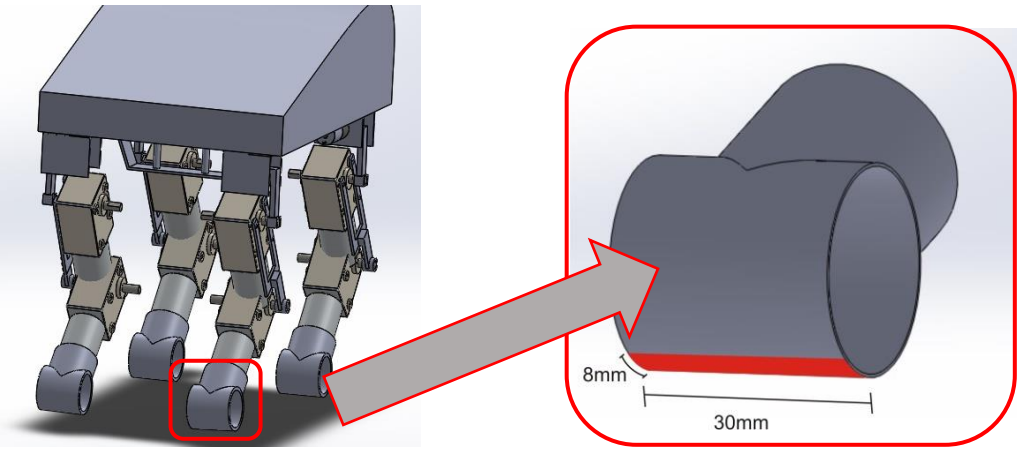

Zero Moment Point concept comprises of the *x* and *y* coordinates. Hence, coordinates are determined by the following equations.

.

$$x_{ZMP} = \frac{\Sigma m_i(\ddot{z}_i + g)x_i - \Sigma m_i \ddot{x}_i z_i}{\Sigma m_i(\ddot{z}_i + g)} \tag{4.1}$$

$$y_{ZMP} = \frac{\Sigma m_i(\ddot{z}_i + g)y_i - \Sigma m_i \ddot{y}_i z_i}{\Sigma m_i(\ddot{z}_i + g)} \tag{4.2}$$

Above equation has variables m_i, g, x_i, y_i, and z_i denotes the mass, gravitational acceleration, and center of gravity coordinates for link *i* respectively. The coordinates equations for model of simple inverted pendulum with single mass are as follow.

$$x_{ZMP} = x_{cg} - \frac{\ddot{x}_{cg} z_{cg}}{\ddot{z}_{cg} + g} \tag{4.3}$$

$$y_{ZMP} = y_{cg} - \frac{\ddot{y}_{cg} z_{cg}}{\ddot{z}_{cg} + g} \tag{4.4}$$

Here, x_{cg} and y_{cg} denotes the center of gravity coordinates for single mass inverted pendulum. As we have not variations in height of the robot trunk. Hence, equations become simple as follow.

$$x_{ZMP} = x_{cg} - \frac{\ddot{x}_{cg} z_{cg}}{g} \tag{4.5}$$

$$y_{ZMP} = y_{cg} - \frac{\ddot{y}_{cg} z_{cg}}{g} \tag{4.6}$$

From the hardware parameters of the robot and trotting gait pattern factors, supporting stripe of ZMP can be illustrated in the figure below.

Figure 4.4

Supporting Stripe of ZMP

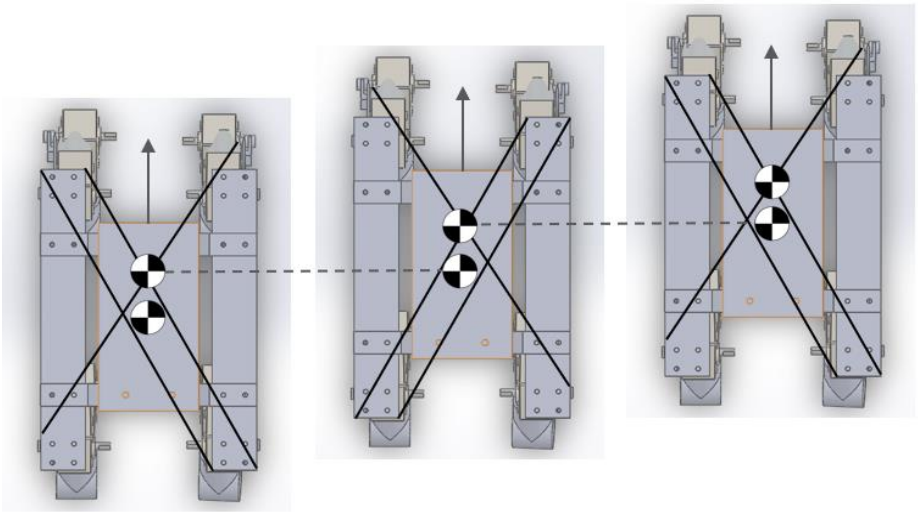

Quadruped robot has trotting gait cycle to move forward or backward. During movement of the robot, ZMP trajectory is controlled to stay in supporting stripe along the longitudinal axis to keep the robot balanced. Center of Mass moves in x-y plane during trotting following the pre-determined trajectory.

4.2.1 Gait Trajectory Tracking using Robust Structured H2 / H∞ Control

Gait pattern is the way of walking adopt by the legged robot for locomotion. In literature, many researchers adopted several gait patterns in legged robots but the most effective in term of stability and speed is trotting gait pattern. In trotting gait pattern, diagonal paired legs move simultaneously. Hence the duty factor is 50% as well as ZMP remains in the supporting stripe to keep the stability of the robot trunk.

Figure 4.5

Trotting Gait Pattern of Quadruped Robot

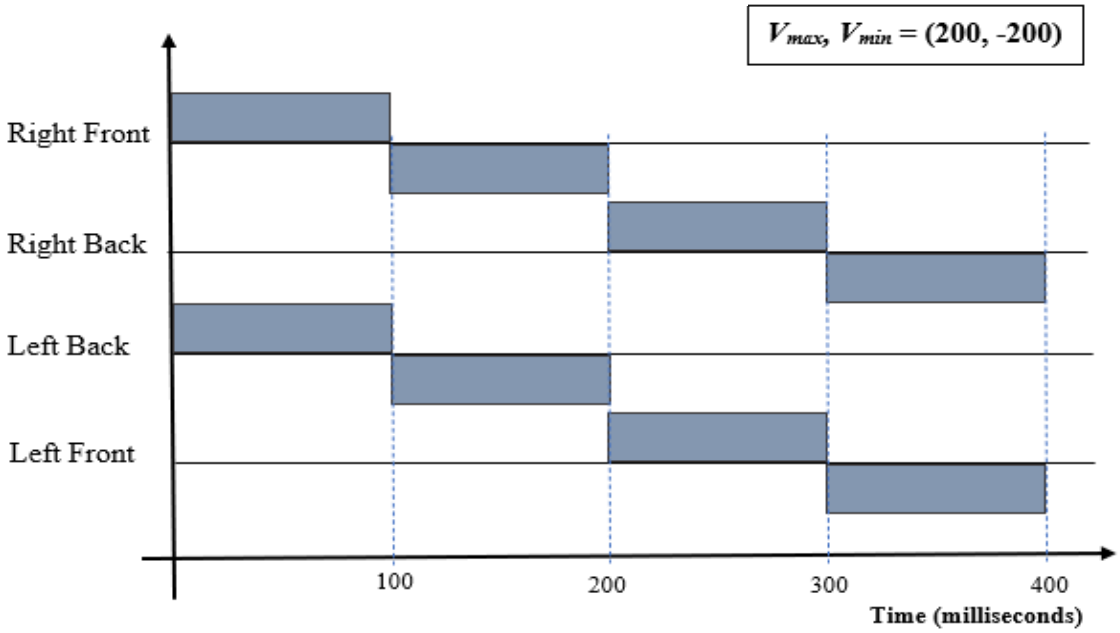

The figure 4.5 present the general trotting git pattern to move in the forward direction and if inverse signal is provided the gait pattern will present the backward motion of the robot. Moreover, the side view of the observed forward motion along with center of mass is presented in figure 4.6. Side view shows that how center of mass shift in longitudinal direction with movement in either forward or backward direction as well as the stance and swing phase of the legs of quadruped robot. In swing phase, the leg leaves the ground as well as in stance phase, leg remain in contact with the ground distinguished by brown and blue colors of legs respectively in figure 4.6.

Furthermore, for controlling the direction of robot in left or right side, trotting gait with another configuration was used. For right turn, LF and RB leg move in forward direction as well as LB and RF leg move in backward direction to turn right side and vice versa.

Figure 4.6

Forward Movement of Quadruped Robot

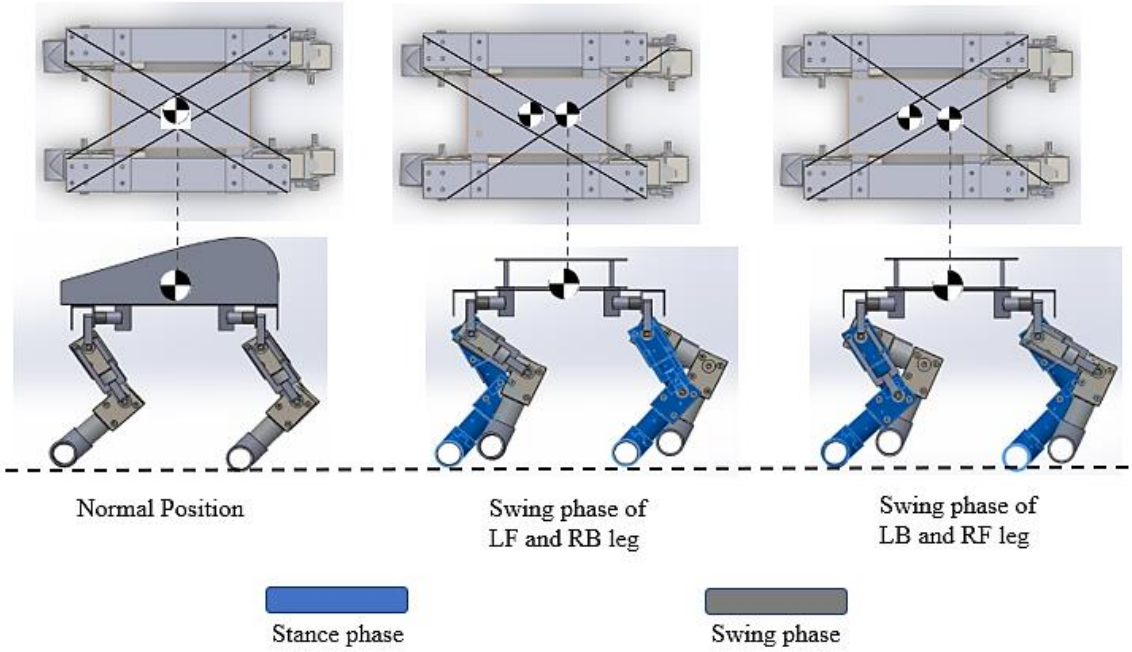

For generating the gait cycle, only shank and thigh section are responsible for motion. Hence, each leg of the robot was considered as two links manipulators, but the hip joint only considered for balancing during walking and against the external disturbances along the lateral directions. Therefore, we considered the two links manipulator control model for the two degree of freedom leg and half sinusoidal pattern for gait as shown in figure below.

Figure 4.7

Kinematics of Each Leg and Half Sinusoidal Gait Pattern

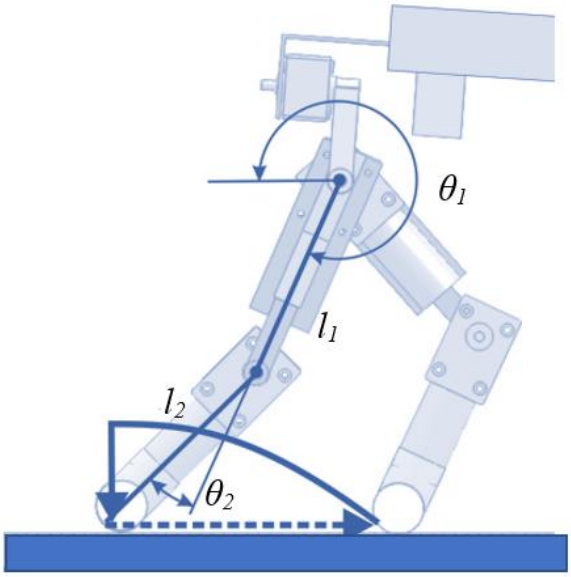

Each leg of robot was modeled as planar two link manipulator as expressed below using Lagrange Equation.

$$M(\theta).\ddot{\theta}+C(\theta,\dot{\theta}).\dot{\theta}+G(\theta)=\tau \tag{4.7}$$

Here, M, C and G represents the Mass, Coriolis and Gravity matrices respectively are given below as well as τ and θ represent the torque and joint position, respectively.

$$M=\begin{bmatrix}(m_1+m_2)l_1^2+m_2l_2^2+2m_2l_1l_2\cos\theta_2 & m_2l_2^2+m_2l_1l_2\cos\theta_2\\ m_2l_2^2+m_2l_1l_2\cos\theta_2 & m_2l_2^2\end{bmatrix} \tag{4.8}$$

$$C=\begin{bmatrix}-m_2l_1l_2(2\dot{\theta}_1\dot{\theta}_2+\dot{\theta}_2^2)\sin\dot{\theta}_2\\ m_2l_1l_2\dot{\theta}_1^2\sin\theta_2\end{bmatrix} \tag{4.9}$$

$$G=\begin{bmatrix}(m_1+m_2)gl_1\cos\theta_1+m_2gl_2\cos(\theta_1+\theta_2)\\ m_2gl_2\cos(\theta_1+\theta_2)\end{bmatrix} \tag{4.10}$$

The system is dynamic coupled and nonlinear. Hence for linearization, feedback linearization control can be applied. A simple PID controller can implement in the absence of disturbances or uncertainties, but in real environment uncertainties may cause the system unstable. Therefore, we need an optimal H2 / H∞ structured specified controller, which is a robust controller and can be used for real time environment in the presence of uncertainties.

Moreover, each joint of the leg is actuated by the DC motor, and each motor has different inertia and uncertainties. Hence, different transfer function will be obtained for each joint i.e., actuator causing motion for shank and thigh respectively. An equivalent model of DC motor is considered as shown below to determine the respected transfer functions.

Figure 4.8

Equivalent Model of DC Motor

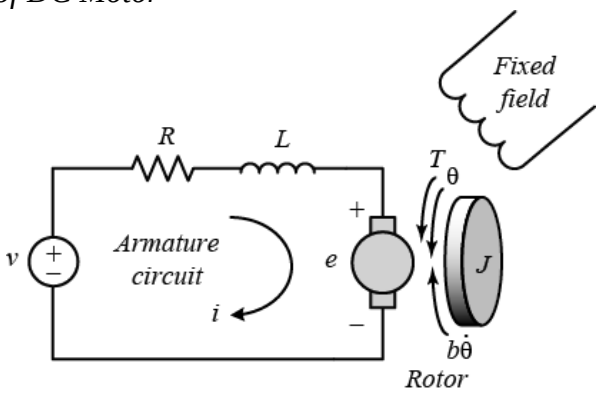

As we know, the armature current (*i*) is directly proportional to torque (T) as well as the back emf (*e*) has direct relation with rotor's velocity ($\dot{\theta}$).

$$T \infty i$$

$$T = Ki \tag{4.11}$$

$$e \infty \dot{\theta}$$

$$e = K\dot{\theta} \tag{4.12}$$

By considering the circuit of DC motor shown in figure 4.8 and substituting the values of equation (4.11) and (4.12), we got the following relations.

$$J\ddot{\theta} + b\dot{\theta} = Ki \tag{4.13}$$

$$L\frac{di}{dt} + Ri = V - K\dot{\theta} \tag{4.14}$$

Hence, transfer function obtained for DC motor is

$$\frac{\theta(s)}{V(s)} = \frac{K}{s((J+b)(L+R)+K^2)} \tag{4.15}$$

Here V, K, *J*, R, b, and L represent the input voltage, constant, rotor inertia, armature resistance, viscous friction constant and armature inductance, respectively.

After substituting the values of motor used to actuate the shank, transfer function obtained as

$$\frac{\theta(s)}{V(s)} = \frac{0.0197}{1.935\,exp{-11}\,s^3 + 1.547\,exp{-05}\,s^2 + 0.0003938\,s} \qquad (4.16)$$

Transfer function for the motor used to actuate the thigh section is obtained as follow.

$$\frac{\theta(s)}{V(s)} = \frac{0.0403}{9.687\,exp{-12}\,s^3 + 7.743\,exp{-06}\,s^2 + 0.0002543\,s} \qquad (4.17)$$

4.2.2 Retrieval Against Sideways Forces -Structured H2 / H∞ Compliant Control

Sideways disturbances retrieval control is along the lateral directions of the robot to stabilize itself using free gait pattern. For implement this control, a simple compass biped robot model is considered to stabilize against the sideway disturbances. Quadruped robot can fell either on any side towards right or left if sufficient external force applied on it. Therefore, robot needs a proper step position using free style sideway gait pattern to bring the body in stable position. Hence, to determine the required position of footstep, law of conservation of angular momentum is used. The below figure represents the configuration of robot's leg when a sideway external force exerts on it until the robot comes to ultimate recovered position.

Figure 4.9

Leg's Configuration of Biped Robot During Retrieval Control

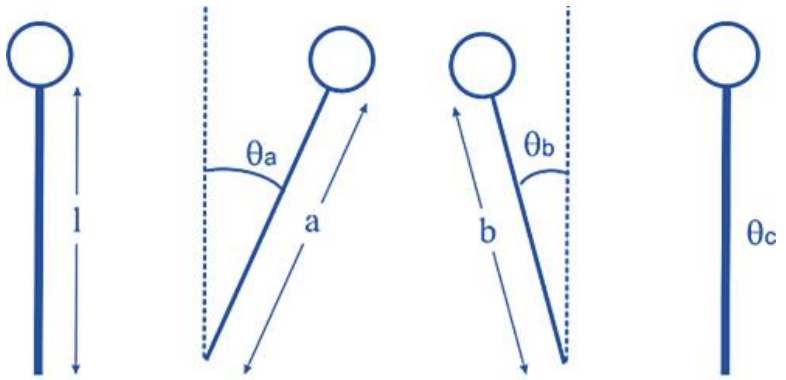

Final position of foot can be seen in above figure,

$$\theta_c = 0 \quad \text{and} \quad \dot{\theta}_c = 0 \tag{4.18}$$

Using equation of angular motion,

$$\frac{\omega_1^2 - \omega_0^2}{2\theta} = \alpha \tag{4.19}$$

Thus, angular acceleration is determined by the following equation.

$$\frac{\dot{\theta}_C^2 - \dot{\theta}_B^2}{2\theta_B} = \ddot{\theta}_B \tag{4.20}$$

Law of conservation of momentum,

$$I_f \omega_f = I_o \omega_o \tag{4.21}$$

$$\dot{\theta}_B = \frac{ml_A^2\dot{\theta}_A \cos(\theta_A + \theta_B)}{ml_B^2} \tag{4.22}$$

$$\dot{\theta}_B = \frac{ml_A^2\dot{\theta}_A(\cos\theta_A \cos\theta_B - \sin\theta_A \sin\theta_B)}{ml_B^2} \tag{4.23}$$

At pivoting of leg B, the final rotation of trunk,

$$ml_B^2\,\ddot{\theta}_B = mgl_B\theta_B \tag{4.24}$$

$$\ddot{\theta}_B = \frac{g\theta_B}{l_B} \tag{4.25}$$

Using equation (4.18), (4.20) and (4.25),

$$\frac{-\dot{\theta}_B^2}{2\theta_B} = \frac{g\theta_B}{l_B} \tag{4.26}$$

Using small angle approximation,

$$\dot{\theta}_B = \frac{ml_A^2\dot{\theta}_A(\cos\theta_A\left(1-\frac{\theta_B^2}{2}\right) - \sin\theta_A\theta_B)}{ml_B^2} \tag{4.27}$$

From (4.26) and (4.27)

$$l_B^2\sqrt{\frac{2g}{l_B}}\theta_B = l_A^2\dot{\theta}_A(2\cos\theta_A - cos\theta_A\theta_B^2 - 2\sin\theta_A\theta_B) \tag{4.28}$$

After simplifying, the above equation becomes.

$$cos\theta_A\theta_B^2 + \left(\frac{l_B^2}{l_A^2\dot{\theta}_A}\sqrt{\frac{2g}{l_B}} + 2\sin\theta_A\right)\theta_B - 2\cos\theta_A = 0 \tag{4.29}$$

Applying small angle approximation, $l_B \approx l$

Where, l represents Height of Center of Mass.

$$l_B = l_A\cos\theta_A \tag{4.30}$$

The minimum and maximum height of robot's trunk can be determined by the following equations respectively,

$$l_{min} = l_B \cos\theta_B - a \sin(90 - \varphi_r) \qquad (4.31)$$

$$l_{max} = l_B \cos\theta_B + a \sin(90 - \varphi_r) \qquad (4.32)$$

Where, a is the perpendicular distance between diagonal line connecting stance hips and swinging hip as well as φ_r is the roll angle of robot's trunk.

Figure 4.10

Configuration of Quadruped Robot During Retrieval Compliant Control

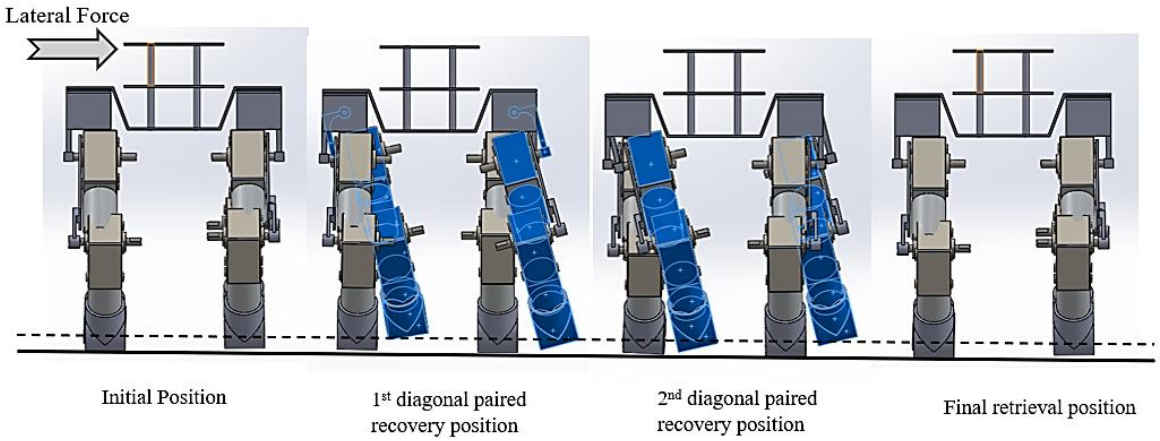

For the implementation of H2/ H∞ robust mixed structured control, the robot is modeled as the simple compass biped robot as follow,

$$M(\theta).\ddot{\theta} + C(\theta,\dot{\theta}).\dot{\theta} + G(\theta) = \tau \qquad (4.33)$$

Like the gait trajectory control, we need to consider the mass, Coriolis, and gravity matrices of biped compass as follow,

$$M = \begin{bmatrix} m_h l^2 + m\left(l^2 + a^2 + b^2 - 2bl\cos\theta_b\right) & mb\left(b - l\cos\theta_b\right) \\ mb\left(b - l\cos\theta_b\right) & mb^2 \end{bmatrix} \qquad (4.34)$$

$$C = \begin{bmatrix} 2mbl(\sin\theta_b)\dot{\theta}_b & mbl(\sin\theta_b)\dot{\theta}_b \\ -mbl(\sin\theta_b)\dot{\theta}_a & 0 \end{bmatrix} \qquad (4.35)$$

$$G = \begin{bmatrix} -g\left(ma + ml + m_h l\right)\sin\theta_a + mb\sin\left(\theta_a + \theta_b\right) \\ gmb\sin\left(\theta_a + \theta_b\right) \end{bmatrix} \qquad (4.36)$$

Where,

m_h : Point mass of biped

m : mass of the leg

l : Length of the leg for two sections (shank and thigh)

θ_a and θ_b : Angular positions of the legs

The designed robot has same length for both sections shank and thigh. Moreover, of hip joints for sideway retrieval are actuated by 4 similar DC motors. For modeling of DC motor, consider the equations (4.13) and (4.14),

$$J\ddot{\theta} + b\dot{\theta} = Ki$$

$$L\frac{di}{dt} + Ri = V - K\dot{\theta}$$

The state space equations of connected links and DC motor used for actuation are given below.

$$\frac{d}{dt}\begin{bmatrix}\ddot{\theta}\\ \dot{\theta}\\ i\end{bmatrix} = \begin{bmatrix}0 & 1 & 0\\ 0 & -\frac{b}{J} & \frac{K}{J}\\ 0 & -\frac{K}{L} & -\frac{R}{L}\end{bmatrix}\begin{bmatrix}\ddot{\theta}\\ \dot{\theta}\\ i\end{bmatrix} + \begin{bmatrix}0\\ 0\\ \frac{1}{L}\end{bmatrix}V \qquad (4.37)$$

$$y = \begin{bmatrix}1 & 0 & 0\end{bmatrix}\begin{bmatrix}\ddot{\theta}\\ \dot{\theta}\\ i\end{bmatrix} \qquad (4.38)$$

The matrices A and B obtained after substituting the parameters are as follow,

$$A = \begin{bmatrix}0 & 1 & 0\\ 0 & \text{-0.7011} & \text{7.5367exp+03}\\ 0 & \text{-8.9883exp+03} & \text{-1.1924exp+06}\end{bmatrix} \qquad (4.39)$$

$$B = \begin{bmatrix}0\\ 0\\ \text{3.1987exp+05}\end{bmatrix} \qquad (4.40)$$

Hence the transfer function obtained as follow,

$$\frac{\theta(s)}{V(s)} = \frac{0.0281}{1.166\text{exp-}11\ s^3 + 1.39\text{exp-}05\ s^2 + 0.0007994\ s} \tag{4.41}$$

4.2.3 Weight Selection

The weights parameters work as tuner/ adjuster of the controller. The sensitivity and the complimentary sensitivity functions can be designed to get the required conditions. In this research, the H2 / H∞ mixed robust controller is used for gait tracking and sideways disturbances retrieval compliant control. The sensitivity function is designed for following the preferred performance, while the complementary sensitivity function is designed by weight that comprises all the possible uncertainties. The basic aim to design H2 / H∞ structured specified controller is to minimize the cost function J_2.

$$J_2 = \int_0^\infty e^2(t)\,dt = E(s)_2^2 \tag{4.42}$$

Using Skogestad's method, the sensitivity weight for shank, thigh and hip motor are selected as follow,

$$W_s(s) = \frac{0.5s + 1}{s + 0.001} \tag{4.43}$$

Figure 4.11

Plot for Sensitivity Weight Inverse (1/Ws)

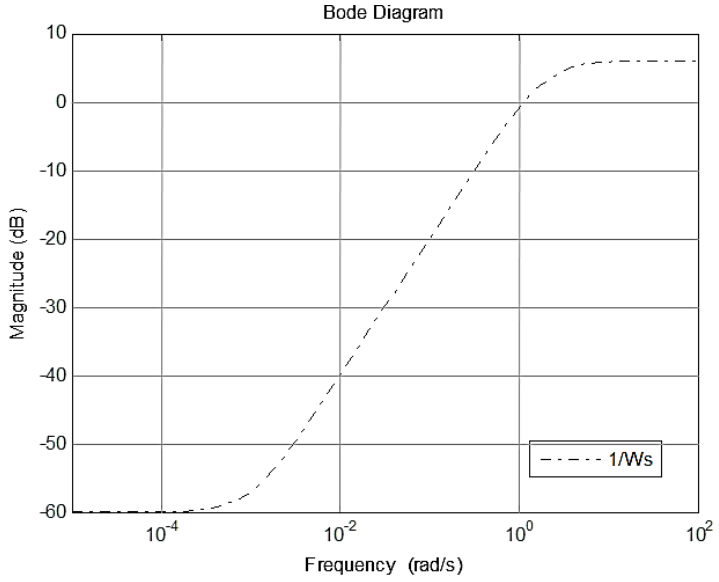

Plot for singular value of sensitivity weight inverse is shown in figure 4.11.

The complimentary sensitivity weights obtained for all three motors of shank, thigh, and hip respectively are given below.

$$W_t(s) = \frac{4.96\,s^2+371.25\,s+240}{s^2+259.9s+1520} \tag{4.44}$$

$$W_t(s) = \frac{4.16\,s^2+25.40\,s+4.65}{s^2+120.4s+285.42} \tag{4.45}$$

$$W_t(s) = \frac{3.28s^2+6.135s+3.93}{s^2+167.8s+246.12} \tag{4.46}$$

The plot for system uncertainty values and complimentary sensitivity weights for shank, thigh and hip motors are presented in figure 4.12, 4.13 and 4.14, respectively.

Figure 4.12

System Uncertainty and Complimentary Sensitive Weight Values for Shank Motor

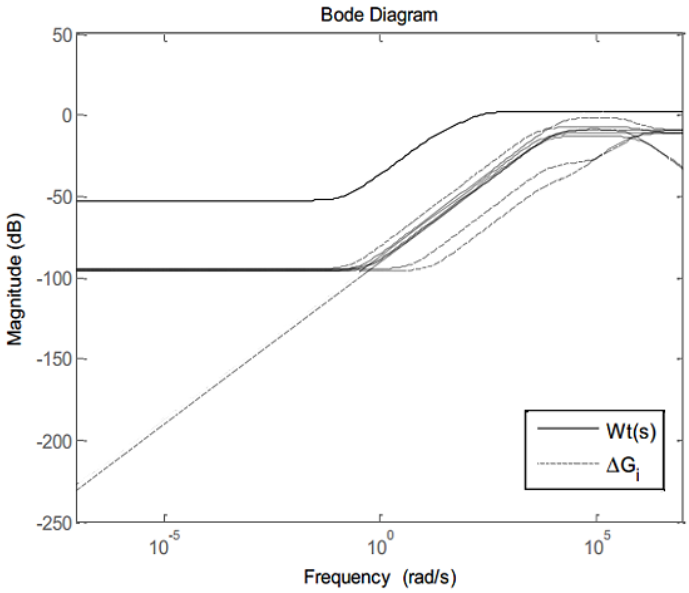

Figure 4.13

System Uncertainty and Complimentary Sensitive Weight Values for Thigh Motor

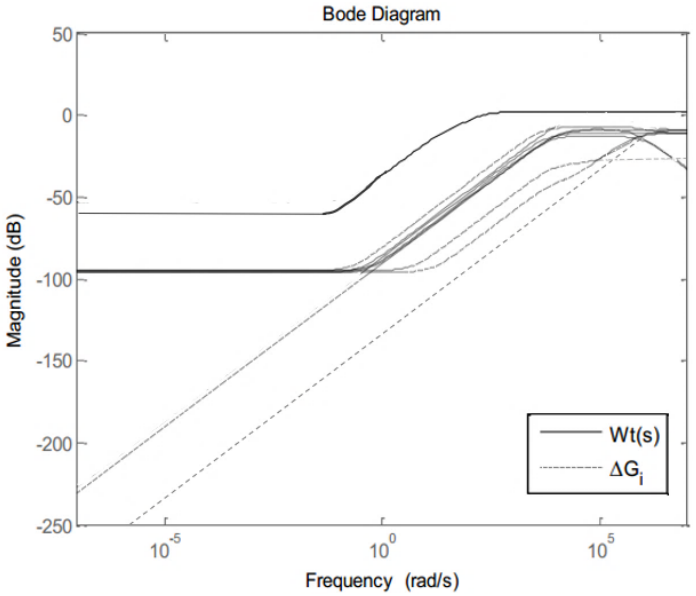

Figure 4.14

System Uncertainty and Complimentary Sensitive Weight Values for Hip Motor

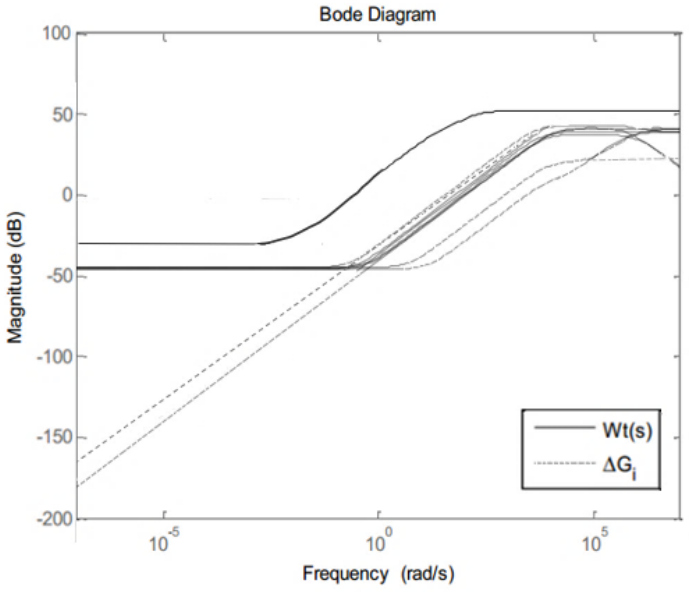

The proposed controller is implemented in the structure of Proportional Integration Derivative (PID) for gait trajectory tracking as well as for sideway disturbances retrieval control.

$$K(s) = K_P + \frac{K_i}{s} + \frac{K_d \,.\, s}{M.s+1} \qquad (4.47)$$

Hence, for both balancing control and sideways disturbances retrieval control, values of parameters including K_P, K_i, K_d, and M were determined by adopting Particle Swarm Optimization (PSO) technique.

PSO is an evolutional technique adopts social behavior like school of fish, or group of birds to optimize the variety of functions. Technique can be illustrated as flow chart in figure 4.15.

Figure 4.15

Flow Chart of Particle Swarm Optimization

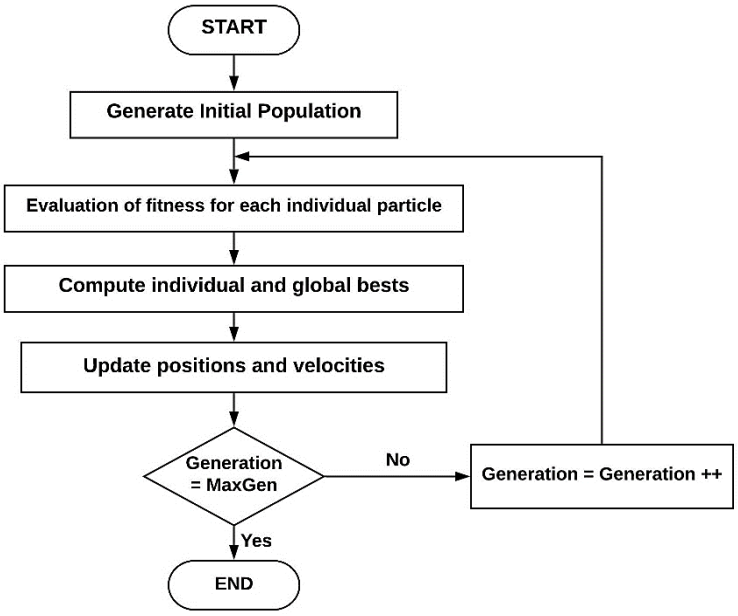

PSO has different variables including position vector $xi = [xi_1, xi_2, \ldots\ldots xi_N]$ and velocity vector $vi = [vi_1, vi_2, \ldots\ldots vi_N]$ for N-Dimensions. The fitness of particle is estimated by objective function of optimization problem. The global best position $G = (g_1, g_2, \ldots, g_N)$ is generated by whole swarm's individual best position. The following two equations use in the PSO technique to update the velocities and positions of particles.

$$v_i(k+1) = w.v_i(k) + c_1.r_1.\big(P_i(k) - x_i(k)\big) + c_2.r_2.(G(k) - x_i(k)) \qquad (4.48)$$

$$x_i(k+1) = x_i(k) + v_i(k) \qquad (4.49)$$

Where;

***w**: Inertia Weight*

***v**: Velocities ranges from [-Vmax to +Vmax] to control unnecessary roaming.*

***c_1 & c_2** : Acceleration coefficients (positive constant)*

***r_1 & r_2**: Random variables ranges [0,1]*

Finally, we got gains and other variable values of PID equation after using Optimization method for balancing control actuators (shank and thigh motor) with the following controlling parameters as determined generation size = 100, swarm size = 10, particle dimensions = 4, c1 =c2 =2, inertia weight changing from 0.8 to 0.5, and velocities ranges from -200 to +200. Thus, two combinations result of parameters for balancing control actuators obtained as follow:

For actuator linked with shank section.

$$K(s) = 4.685 + \frac{0.0423}{s} + \frac{0.256\ \ s}{0.000289\,s+1}$$

With $J_{\infty,a} = 0.454$, $J_{\infty,b} = 0.751$, and $J_2 = 0.0648$

Similarly, for actuator linked with thigh section.

$$K(s) = 3.95 + \frac{0.00313}{s} + \frac{0.541\ \ s}{0.00079\,s+1}$$

With $J_{\infty,a} = 0.641$, $J_{\infty,b} = 0.810$, and $J_2 = 0.01287$

Consequently, the two controlling parameters for hip motor (being used for sideway retrieval control) are different from the parameters used for other two motors. Swarm size =20 and velocity ranges from -120 to +120. And the combination results obtained for this motor are as follow.

$$K(s) = 2.0665 + \frac{0.7569}{s} + \frac{0.2856\ \ s}{0.00029\,s+1}$$

With $J_{\infty,a} = 0.511$, $J_{\infty,b} = 0.694$, and $J_2 = 0.0481$

4.3 Navigation Control of Quadruped Robot

Navigation control itself is a wide and diverse control in term of localization, path optimization and mapping. For this project, we used an open loop feedback control of navigation from one initial point to final point by approximation method. The distance covered by the system was approximated by the number of steps required to cover the unit distance. This method is not absolute, but error is very less about 2-3%.

Figure 4.16

Navigation Control of Quadruped Robot

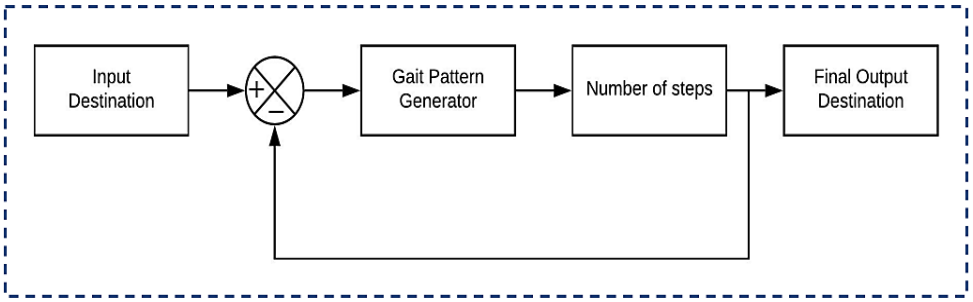

For navigation control, an android application was developed in android studio using java and CSS language. The android application has different modes to operate the robot including manual mode and auto mode. In manual mode, robot moves according to the instructions from joystick panel. While, in auto mode user can input the instructions to move the robot from an initial point to the destination point and robot reached to the destination by itself in autonomous mode. The application developed for the robot control remotely or autonomously is shown in figure below.

Figure 4.17

Android Application Developed for Quadruped Robot Control

CHAPTER 5
SIMULATION AND EXPERIMENTAL RESULTS

5.1 Simulations of Balancing and Retrieval Control

Simulation of the actuators used for the quadruped robot was performed on MATLAB software. Each leg has 3 degree of freedom (3 actuators) motors at knee and hip for shank section, thigh section and lateral movements, respectively. Hence for each motor we implemented the robust control in MATLAB to observe the responses of motors using Arduino controller between actuators and MATLAB. Firstly, the motor attached at knee for shank section interfaced to control using H2 / H∞ controller in structure of PID in MATLAB. The response of motor can be seen in figure below.

Figure 5.1

Simulation of Knee Joint Motor

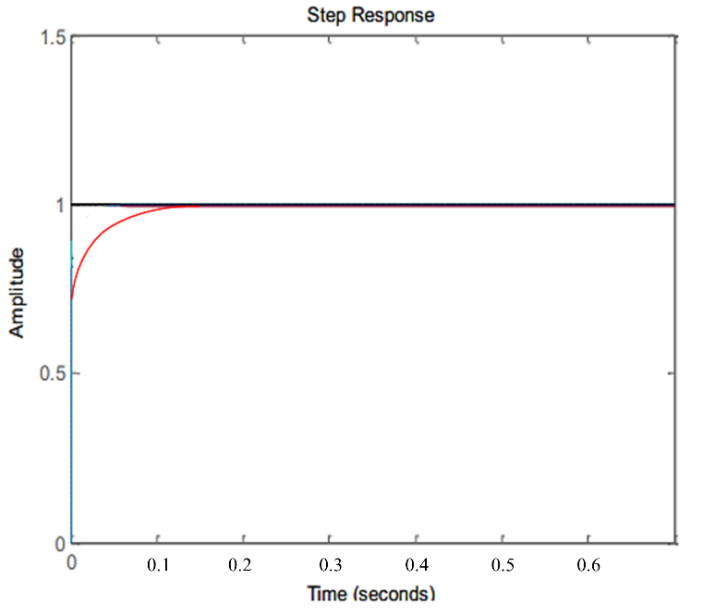

Figure 5.2

Simulation of Hip Motor for Thigh Link

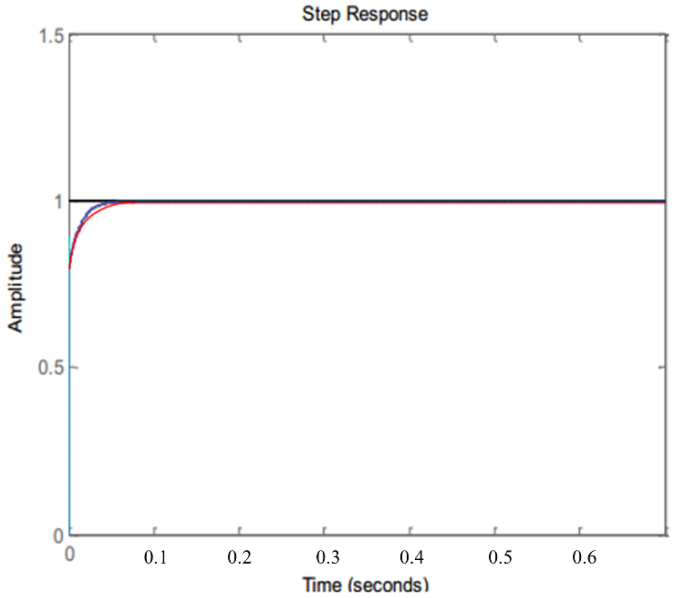

Similarly, the simulation for Hip motor using for lateral motion in sideway retrieval control was performed on MATLAB. But for this motor, two different controls i.e., well-tuned PID as well as the H2 / H∞ robust control was implemented to determine the differences under uncertainties. because literature research presents that PID control is easier and gives better performance without uncertainties. Hence, under uncertainties the response is different in terms of overshoot and settling time.

Figure 5.3

Simulation of Hip Motor using Well Tunned PID Control

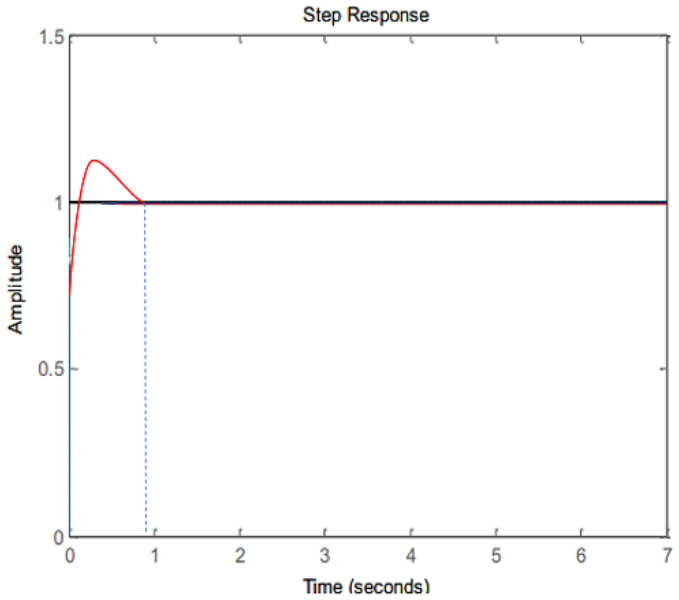

Figure 5.3 shows the simulation of actuator using well-tuned PID control under uncertainties, the settling time for PID control is about 0.9 seconds but in robust control the settling time is about 0.55 seconds and overshoot is also very small as compared to the PID control. Moreover, there is no steady state error, and the settling as well as the rising time are satisfactory for robust control under uncertainties.

Figure 5.4

Simulation of Hip Motor using Robust H2/H∞ Compliant Control

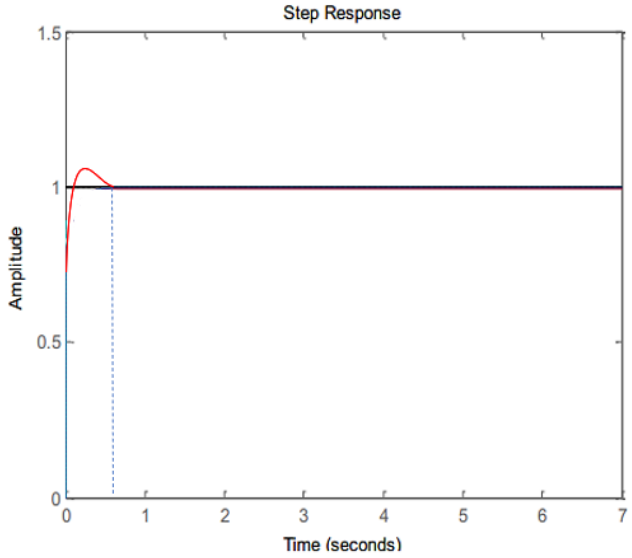

5.2 Experimental Results

5.2.1 *Gait Tracking and Balancing Control*

Experimental results are obtained directly from the Arduino controller using serial monitor. Basic two experiments were conducted for gait tracking and retrieval control. Experimental results obtained in response to the balancing of the robot and throughout trotting in rough carpet terrain as well as on smooth tiles is shown in figures below, which represents the roll and pitch angles.

Figure 5.5

Trunk Behavior While Trotting on Smooth Tiles

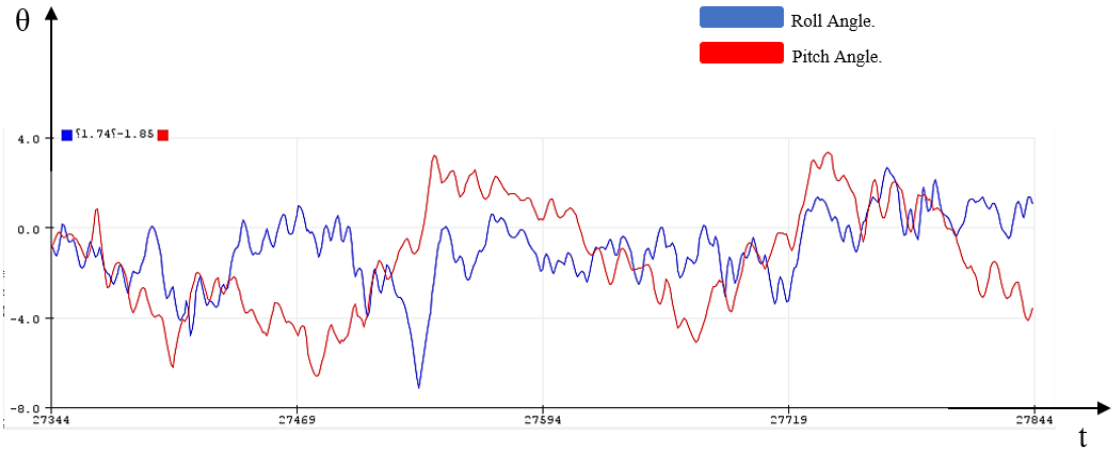

Figure 5.6

Trunk Behavior While Trotting on Rough Carpet

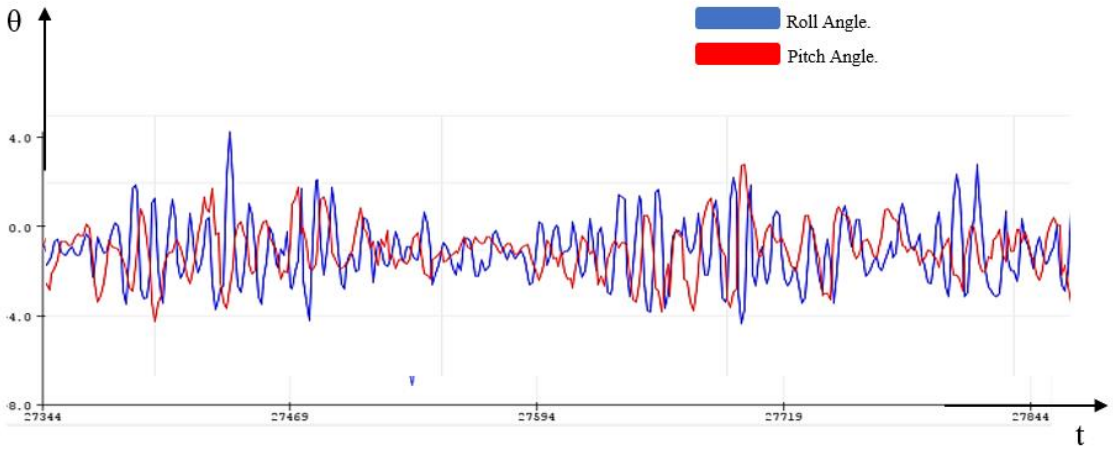

Figure 5.5 represents the trunk behavior of quadruped robot while trotting on the smooth surface (tiles). The fluctuations in the roll angle lies between 2.5 to -7.0 degrees and pitch angle lies between 3.5 to -6.0 degrees. Figure 5.6 shows the attitude of robot trotting through rough carpet. The angle fluctuations for roll and pitch lie between ±4.0 degrees and 3.5 to -4.0 degrees, respectively. Moreover, the robot can trot stably on various surfaces using the balancing algorithm with proposed gait tracking control.

Figure 5.7

Real Time Forward Walking of Quadruped Robot

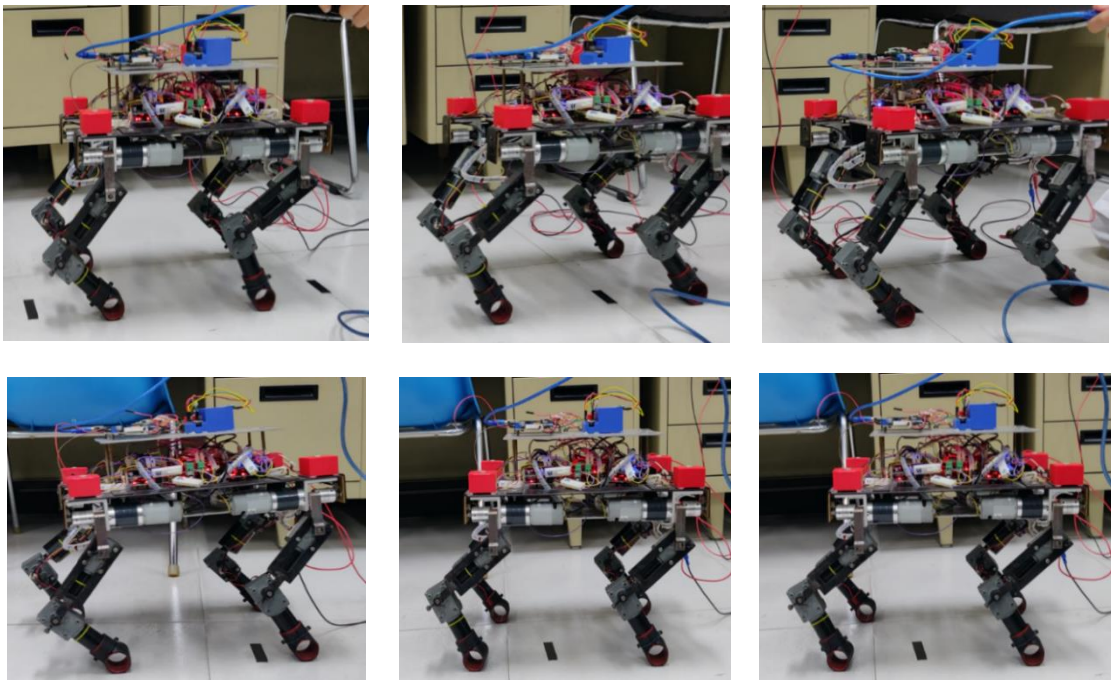

5.2.2 *Retrieval Compliant Control Results*

For retrieval control against sideway lateral forces, we conducted experiment in both directions left and right. In this approach, when lateral force act on the robot in any direction, the robot tries to recover its foot position to maintain the balance of the body using free gait pattern. To determine the lateral force, IMU unit comprises of accelerometer is used to determine the accelerations produced in the body by exerting force along with the change in the orientation of the body.

Figure 5.8

Roll and Pitch Angles During Lateral Force Towards Left Side of Quadruped Robot

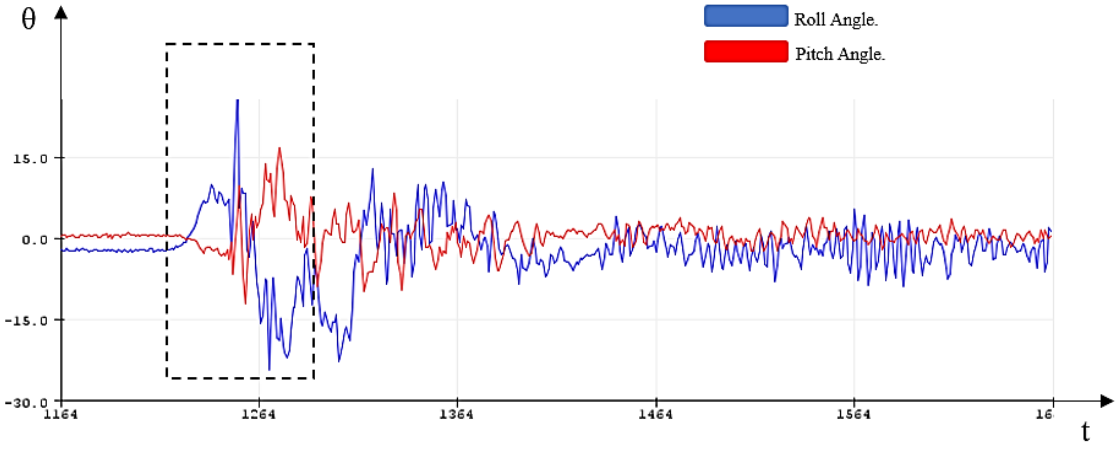

Figure 5.9

Roll and Pitch Angles During Lateral Force Towards Right Side of Quadruped Robot

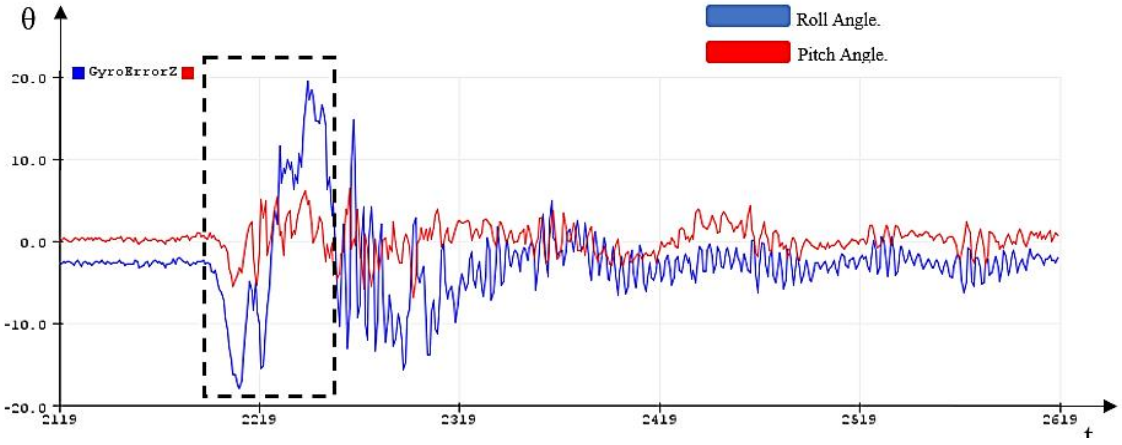

Figure 5.8 presents the roll angle of the robot, when lateral force acts towards left side of the robot. The robot retrieves its foot position to maintain the stability of the body and move towards left side using free gait pattern. Consequently, figure 5.9 shows the roll angle when lateral force exerts on the trunk from left to right direction. The robot tries to keep its body in stable position by moving towards right direction.

Figure 5.10

Retrieval of Footstep Towards Left Side to Maintain its stability

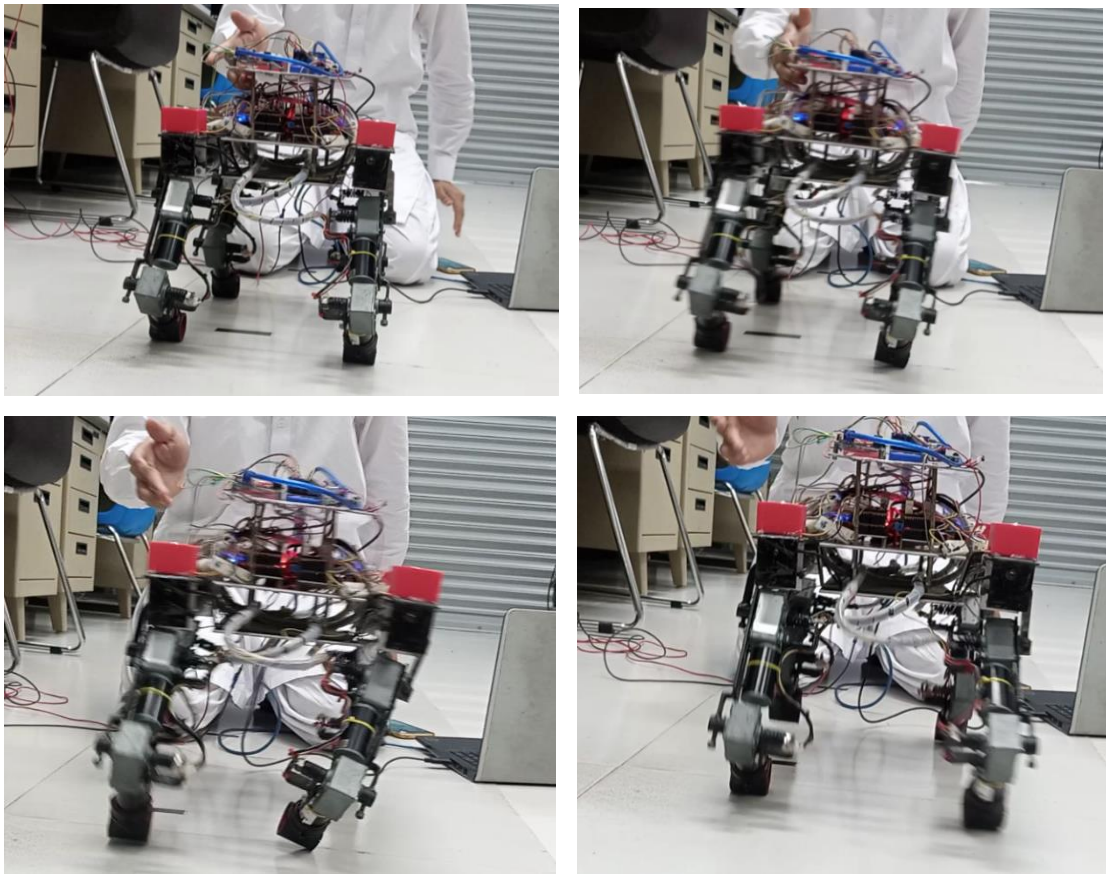

CHAPTER 6
CONCLUSION AND FUTURE WORK

Quadruped robot developed at AIT has ability of dynamic walking using trotting gait pattern. It can move forward, right, and left turn as well as it can trot on same location. The quadruped used the balancing control algorithm (ZMP) along with trotting gait trajectory tracked by utilizing proposed H2/ H∞ mixed structured robust control. Simulation performed on MATLAB confirms that system response in following the step input is satisfactory as well as there is no steady state error. Moreover, the overshoot and settling time is small as compared to period of gait cycle. Simulation demonstrates that settling time in both actuators of each leg being used in balancing control is less than 0.3 seconds and overshoot is negligible.

The proposed robust control performed very well in tracking the gait trajectory. Experiments performed on two different surfaces i.e., smooth tiles and rough carpet, demonstrates that angle variations are ±7 degrees and ±4 degrees, respectively. Moreover, the pitch angle variations in trunk of robot are less as compared to roll angles. Hence, the robot can stably walk using trotting pattern on different surfaces keeping itself balanced.

Secondly, most important objective is to retrieval of foot position against the lateral forces disturbance to keep the body stable using free gait pattern. The proposed compliant control is also same robust H2 / H∞ mixed structured control used to determine the foot position against lateral forces to avoid falling. Simulation shows that settling time is less than 0.6 seconds and overshoot is also very small as compared to well-tuned PID controller along with no steady state error. Experimental results illustrate that trunk takes less than 2 second to retrieve its foot position and stable itself.

Thirdly, Navigation control is implemented in the robot which is almost open loop feedback system. In this control, robot can move to the defined destination autonomously, but has some error about less than 3% and it is acceptable. Moreover, robot can operate remotely using mobile application.

In research culture, there always remains modifications and further advancement. For recommendations, quadruped robot using light weight material and BLDC motors

equipped with planetary gears can develop for future research to implement more advance features in the robot i.e., jumping and climbing etc. Moreover, a new configuration of hip motor being used for lateral motion can increase the joint angle workspace.

REFERENCES

Arikawa, K., & Hirose, S. (1996). Development of quadruped walking robot TITAN-VIII. *Proceedings of IEEE/RSJ International Conference on Intelligent Robots and Systems. IROS '96* (pp. 208-2141). Osaka, Japan: IEEE.

Ding, Y., & Park, H.-W. (2017). Design and experimental implementation of a quasi-direct-drive leg for optimized jumping. *2017 IEEE/RSJ International Conference on Intelligent Robots and Systems (IROS)* (pp. 300-305). Vancouver, BC, Canada: IEEE.

F. García-Cárdenas, N. S. (2020). Charlotte: Low-cost Open-source Semi-Autonomous Quadruped Robot. *IEEE International Conference on Autonomous Robot Systems and Competitions (ICARSC).* Ponta Delgada, Portugal: IEEE.

Garcia, E., & Santos, P. G. (2006). On the Improvement of Walking Performance in Natural Environments by a Compliant Adaptive Gait. *IEEE* .

Haldane, D. W., Yim, J. K., & Fearing, R. S. (2017). Repetitive extreme-acceleration (14-g) spatial jumping with Salto-1P. *2017 IEEE/RSJ International Conference on Intelligent Robots and Systems (IROS)* (pp. 3345-3351). Vancouver, BC, Canada: IEEE.

Hutter, M., Gehring, C., Jud, D., Lauber, A., Bellicoso, C. D., Tsounis, V., . . . Bodie, K. (2016). ANYmal - a highly mobile and dynamic quadrupedal robot. *2016 IEEE/RSJ International Conference on Intelligent Robots and Systems (IROS)* (pp. 38-44). Daejeon, South Korea: IEEE.

Kau, N., Schultz, A., Ferrante, N., & Slade, P. (2019). Stanford Doggo: An Open-Source, Quasi-Direct-Drive Quadruped. *2019 International Conference on Robotics and Automation (ICRA)* (pp. 6309-6315). Montreal, QC, Canada: IEEE.

Kitano, S. H. (2016). TITAN-XIII: sprawling-type quadruped robot with ability of fast and energy-efficient walking. *Springer*.

Lakatos, D., Federigi, Y., Gumpert, T., Henze, B., Hermann, M., Loeffl, F., . . . Alin. (2019). A Coordinate-based Approach for Static Balancing and Walking Control of Compliantly Actuated Legged Robots. *2019 International*

Conference on Robotics and Automation (ICRA) (pp. 9509-9515). Montreal, QC, Canada: IEEE.

Lakatos, D., Federigi, Y., Gumpert, T., Henze, B., Hermann, M., Loeffl, F., . . . Seidel, D. (2019). A Coordinate-based Approach for Static Balancing and Walking Control of Compliantly Actuated Legged Robots. *2019 International Conference on Robotics and Automation (ICRA).* Montreal, QC, Canada: IEEE.

Lee, Y. H., Lee, Y. H., Lee, H., Kang, H., Lee, J. H., Phan, L. T., . . . Don. (2020). Development of A Quadruped Robot System with Torque-Controllable Modular Actuator Unit. *IEEE Transactions on Industrial Electronics*, 1-1.

Li, X., Gao, J., Duan, X., Huang, Q., Li, H., Liu, H., . . . Sun, W. (2013). Mechanical design of the legs of hydraulically actuated quadruped bionic robot. *2013 ICME International Conference on Complex Medical Engineering.* Beijing, China: IEEE.

Nguyen, Q., Powell, M. J., Katz, B., Carlo, J. D., & Kim, S. (2019). Optimized Jumping on the MIT Cheetah 3 Robot. *2019 International Conference on Robotics and Automation (ICRA)* (pp. 7448-7454). Montreal, QC, Canada: IEEE.

Vo-Gia Loc, I. M. (2012). Body Workspace of Quadruped Walking Robot and its Applicability in Legged Locomotion. *Journal of Intelligent & Robotic Systems*, 67.

Wait, K. W., & Goldfarb, M. (2014). A Pneumatically Actuated Quadrupedal Walking Robot. *IEEE/ASME Transactions on Mechatronics*, 339-347.

Wait, K. W., Dalley, S. A., & Goldfarb, M. (2008). Design and control of a biomimetic hexapedal walker. *2008 2nd IEEE RAS & EMBS International Conference on Biomedical Robotics and Biomechatronics* (pp. 270-275). Scottsdale, AZ, USA: IEEE.

APPENDICES

APPENDIX A
ENGINEERING DRAWING OF ROBOT'S PARTS

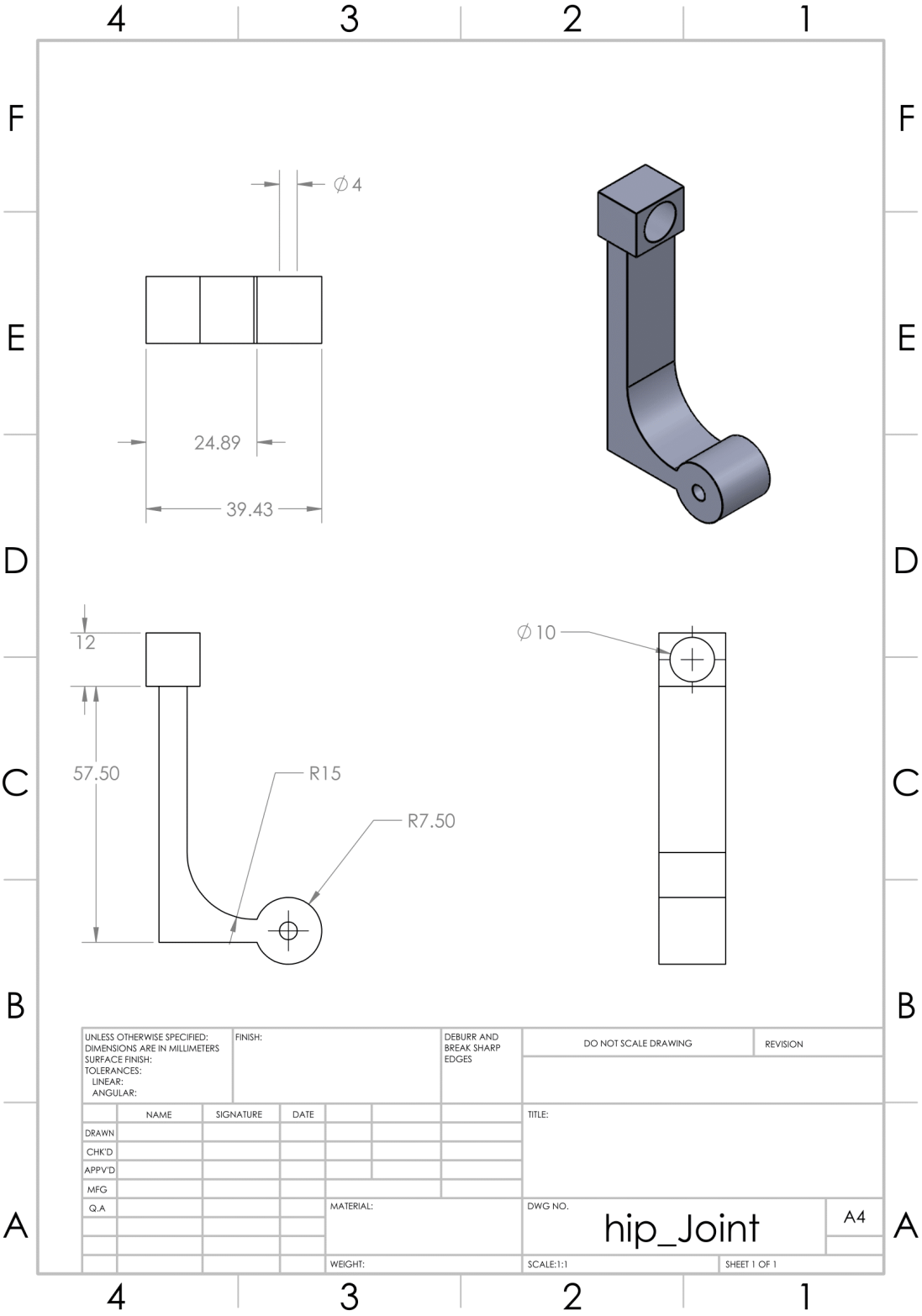

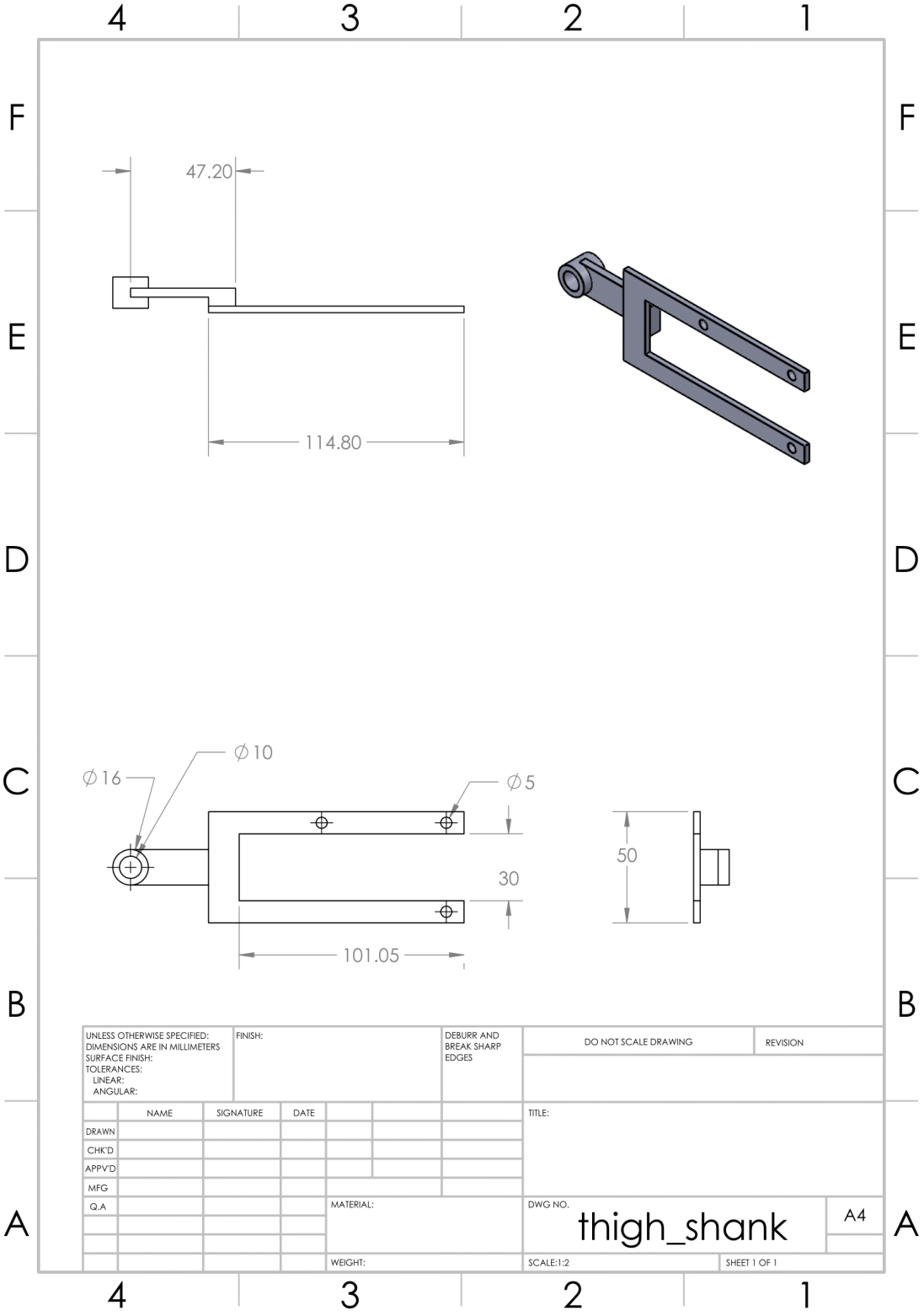
4
3
2
1
F
E
D
C
B
A
47.20
114.80
Ø16
Ø10
Ø5
30
50
101.05
UNLESS OTHERWISE SPECIFIED:
DIMENSIONS ARE IN MILLIMETERS
SURFACE FINISH:
TOLERANCES:
LINEAR:
ANGULAR:
FINISH:
DEBURR AND BREAK SHARP EDGES
DO NOT SCALE DRAWING
REVISION
NAME
SIGNATURE
DATE
DRAWN
CHK'D
APPV'D
MFG
Q.A
TITLE:
MATERIAL:
DWG NO.
thigh_shank
A4
WEIGHT:
SCALE:1:2
SHEET 1 OF 1

APPENDIX B
ENGINEERING DRAWING OF QUADRUPED ROBOT